Lehigh University
Lehigh Preserve

Theses and Dissertations

1-1-1983

Characterization and measurement of noise in optical receivers.

Thanh Van Nguyen

Follow this and additional works at: http://preserve.lehigh.edu/etd

🌀 Part of the Electrical and Computer Engineering Commons

Recommended Citation

CHARACTERIZATION AND MEASUREMENT
OF NOISE IN OPTICAL RECEIVERS

by

Thanh Van Nguyen

A Thesis

Presented to the Graduate Committee

of Lehigh University

in candidacy for the Degree of

Master of Science

in

Electrical and Computer Engineering Department

Lehigh University

1983

ProQuest Number: EP76741
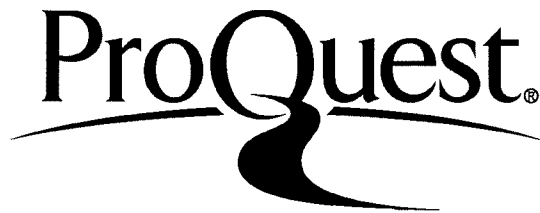
ProQuest.

ProQuest EP76741

This thesis is accepted and approved in partial fullment of
the requirements for the degree of Master of Science

May 13, 1983
　　(date)

ᵛ Professor in Charge

Chairman of the Department

ACKNOWLEDGEMENTS

TABLE OF CONTENTS

LIST OF TABLES

LIST OF FIGURES

List of Symbols

G_O	Midband voltage gain value of the post-amplifier
$E(f)$	Equalizer frequency response
E_O	Midband value of equalizer response
f	Frequency
f_C	Flicker noise corner value
f_H	System high frequency cut-off value
f_L	System low frequency cut-off value
$F(f)$	Filter frequency response
F_O	Midband value of filter response
g_m	Transconductance value of the front-end transistor
h	Planck's constant
i	Summation index
$i_{b'}$	Equivalent input noise current generator of the spreading resistance
i_{dn}	Noise current generator resulting from the dark current plus the leakage current of the p-i-n diode
i_D	Noise current generator of the drain resistor
i_{eq}	Total equivalent input noise current generator of the receiver
i_F	Noise current generator of the feedback resistor
i_{in}	Input noise current generator of the front-end transistor
i_{out}	Output noise current generator of the front-end transistor
i_{ph}	Photo current generator of the p-i-n diode
i_{qu}	Noise current generator resulting from the photo current of the p-i-n diode (Quantum noise)
$\langle i_*^2 \rangle$	Mean square value of a current source
$\langle i_*^2 \rangle^{1/2}$	Root mean square value of a current source

$\dfrac{d\langle i_*^2\rangle}{df}$	Spectral density of a current source
I_B	Average base current of a BJT
I_C	Average collector current of a BJT
I_{dn}	Average noise of the p-i-n diode (dark current current plus leakage current)
I_{gt}	Average gate leakage current of a FET
I_{ph}	Average photo-current generated by the p-i-n diode
k	Boltzmann's constant; current scale factor
n	Number of data points
P	Channel noise factor of a FET
$\bar{P}$	Average value of received optical power
$P_*(f)$	Power spectrum of a voltage source
q	Electronic charge
Q	Statistics variable indicates the disagreement between observation and expectation values; correlation noise factor of a FET
$r_{bb'}$	Spreading resistance of the front-end transistor
$r_{b'e}$	Base-emitter resistance of the front-end transistor
r_{ds}	Drain-source resistance of the front-end transistor
R	Induced gate noise factor of a FET
R'	Input loading as seen by the spreading resistance voltage noise generator
R''	Effective input resistance
R_D	Drain resistor
R_F	Feedback resistor
R_L	Loading resistor for the reference diode
R(f)	Preamplifier transimpedance gain
R_O	Midband value of the transmimpedance gain

$$\frac{d\langle i_*^2\rangle}{df}$$ Spectral density of a current source

I_B Average base current of a BJT

I_C Average collector current of a BJT

I_{dn} Average noise of the p-i-n diode (dark current current plus leakage current)

I_{gt} Average gate leakage current of a FET

I_{ph} Average photo-current generated by the p-i-n diode

k   Boltzmann's constant; current scale factor

n   Number of data points

P   Channel noise factor of a FET

$\bar{P}$ Average value of received optical power

$P_*(f)$ Power spectrum of a voltage source

q   Electronic charge

Q   Statistics variable indicates the disagreement between observation and expectation values; correlation noise factor of a FET

$r_{bb'}$ Spreading resistance of the front-end transistor

$r_{b'e}$ Base-emitter resistance of the front-end transistor

r_{ds} Drain-source resistance of the front-end transistor

R   Induced gate noise factor of a FET

R'   Input loading as seen by the spreading resistance voltage noise generator

R''   Effective input resistance

R_D Drain resistor

R_F Feedback resistor

R_L Loading resistor for the reference diode

R(f)   Preamplifier transimpedance gain

R_o Midband value of the transmimpedance gain

V_{out} Output signal voltage

$\langle v_*^2 \rangle$ Mean square value of the output signal voltage

z_1 Input impedance of a transistor

z_2 Feedback impedance of a transistor

z_3 Output impedance of a transistor

$W(f)$ Weighting function determined by system response

Γ Excess channel noise factor of a FET

η Quantum efficiency of the p-i-n diode

λ Wavelength of light

ν Frequency of light

CHARACTERIZATION AND MEASUREMENT
OF NOISE IN OPTICAL RECEIVERS

by

Thanh Van Nguyen

ABSTRACT

An analysis of noise in optical receivers is presented.
The equivalent input current noise of a p-i-n FET receiver
and a p-i-n BJT receiver are theoretically derived. From
theory, the equivalent input current noise of a receiver can
be expressed as a frequency-dependent polynomial which has
coefficients determined by circuit parameters. The
characterization of all noise sources is therefore possible
by measuring the input noise spectral density. The
measurement is done by using a desk-top computer to control
an automatic spectrum analyzer, a synthesized signal
generator and an analog laser transmitter to measure the
transimpedance spectrum and the output voltage noise
spectrum of the receiver under examination. The equivalent
input current noise spectral density is then obtained by
dividing the output noise voltage spectrum by the
transimpedance spectrum. Good agreement is found between
the measured noise and the noise predicted on the basis of
the respective circuit models. By integrating the
equivalent input noise spectral density of the receiver, the
mean square value of the equivalent total input current
noise is determined. The sensitivity of the receiver as a

function of digital transmission bit rate predicted from both theoretical values and measured values of noise compares favorably with actual measured sensitivities.

For example, in the case of the p-i-n FET receiver, theory predicts that the minimum detected optical power to achieve one error per billion bits of digital transmission at the baud rate of 45 Mb/s is -50.6 dBm. This agrees with the result expected if based upon input noise measurement (i.e., -50.4 dBm). However, actual digital transmission measurement with a non-ideal system filter gives -49.3 dBm.[11] For the p-i-n BJT receiver, at the baud rate of 300 Mb/s, the three values are -37.0 dBm, and -36.8 dBm, and -36.5 dBm,[10] respectively.

CHARACTERIZATION AND MEASUREMENT
OF NOISE IN OPTICAL RECEIVERS

by

Thanh Van Nguyen

SECTION 1.   INTRODUCTION

Since glass fibers with zero dispersion and minimal absorption at a wave-length of about 1.3μm have become available, this wave-length region has attracted growing interest.   The goal of a communication system designer is to create as powerful as possible a transmitter and as sensitive as possible a receiver which operate at this wave-length.   This maximizes the repeater spacing and thus minimizes the transmission cost.   Of course, the reliability issue is also a main concern.

In the design of an optical receiver, the most fundamental limitation of the receiver performance is noise. Noise is the spontaneous fluctuation of current and voltage intrinsic to electronic circuits.   (We will not discuss the extrinsic noise caused by electro-magnetic interference.) For the semiconductor optical receiver, there are four main noise sources:

i.   Quantum noise resulting from the randomness associated with the generation of electron-hole pairs exited by the incident optical radiation.

ii. Flicker noise (or 1/f noise) resulting from the slow fluctuations in conductivity of the semiconductor material. (This type of noise is usually treated as part of the total semiconductor device noise; e.g., see eq. 7, below.)

iii. Shot noise resulting from the random crossing of a junction (potential barrier) by electrical carriers (electrons or holes),

iv. Johnson (or thermal) noise resulting from the random thermal motion of the current carriers.

In order to create as sensitive as possible a receiver, all the above listed noise sources with the exception of quantum noise, which is fundamental in nature, should be minimized by choosing the optimum circuit parameters.

For receivers which operate at 1.3μm wave-length, the most popular circuit configuration is a p-i-n photo-detector coupled to a low noise transimpedance pre-amplifier which has either a micro-wave Field Effect Transistor (FET) or a micro-wave Bipolar Junction Transistor (BJT) at its front-end amplifier. The reason behind this configuration is the lack of high quality 1.3μm Avalanche Photo Diodes (APDs), which can otherwise provide the immediate conversion gain of light power into electrical current prior to transistor amplification. Also, the transimpedance pre-amplifier is

chosen because it has a wider operating bandwidth and a larger dynamic range than its counterpart, the high impedance (or shunt impedance) amplifier. Micro-wave transistors which inherit high figure of merit (g_m/C) are chosen for low noise and good performance at high frequency. A FET front-end is typically used for low operating bandwidth where its noise contribution is proven to be less than that of a BJT front-end.[2] Due to superior reliability and well-known technology, most of the present applications at transmission rates greater than 90 Mb/s employ a BJT front-end amplifier.

In this paper, the equivalent input current noise of two specific receivers will be theoretically derived and practically measured. The results are used to generate accurate noise models for the receivers under examination.

SECTION 2. THEORETICAL NOISE MODELS

As was previously mentioned, the ultimate performance of a communication system is usually set by noise present at the input of the receiver. Noise degrades the signal and impairs the system performance. In an optical receiver, the essential sources of noise are associated with the detection and amplification processes. Understanding the origin, characteristics and interplay of the various noise sources is essential to the design and evaluation of any optical communication system.

2.1 - Optical Detection Techniques

The relative importance of various noise sources in receivers depends very much on the method of demodulation. The two basic methods of demodulating an optical signal are:[6]

1. Direct detection in which the output signal of the receiver is a linear function of the incident optical power.

2. Heterodyne detection in which the incoming optical signal is mixed with a coherent local oscillator to produce a difference frequency from which information is extracted.

Heterodyne detection which is applicable only to single mode transmission, does not appear to be practical for fiber systems at present, because stable single-frequency lasers are required for both carrier generators and local oscillators. Direct detection, however, is simple to implement, the incoming optical signal can be either incoherent or coherent, and the performance of the receiver is independent of the polarization state or the modal content of the optical signal. Therefore, direct detection is the presently preferred method of detection for optical fiber communication systems.

2.2 - Noise Sources in Direct Detection Technique

In figure 1, the various noise sources associated with the detection and amplification processes in an optical receiver employing the direct detection technique are shown. The background radiation noise, which is important in an atmospheric propagation system, is negligible in a fiber system. The beat noise generated in the detector from the various spectral components of an incoherent carrier such as that from a Light Emitting Diode (LED), is negligible when a laser source is used.

Any photo detector has shot noise contribution from the dark current and the leakage current. Also, there is a contribution of the quantum noise which results from the average photo-current. These noise contributions have the same mathematical expression and are characterized by Poisson statistics.[13] The dark current noise and the leakage current noise can be reduced by careful design and fabrication of the detector.[14] The quantum noise, on the other hand, is fundamental in nature and sets the ultimate limit in the receiver sensitivity.[1,2]

Amplifier noise is the combination of thermal noise and shot noise in receivers utilizing a BJT front-end (e.g., eq. 4, 8 and 9), or the combination of thermal noise, coupling noise, channel noise and flicker noise in receivers utilizing a FET front-end (e.g., eq. 4, 6 and 7). Amplifier

noise can be minimized by choosing the optimal circuit parameters.[2]

2.3 - Typical Receiver Noise Modelling

To study these noise sources in detail, two specific receiver configurations are chosen. One is the 1.3μm p-i-n FET optical receiver which was reported by Ogawa in 1979,[8] the other is the 1.3μm p-i-n BJT optical receiver which is under development for high bit rate transmission systems within the Bell Laboratories. Fig. 2 and Fig. 3 show the receiver circuit diagrams and Fig. 4 and Fig. 5 show the theoretical noise models for these receivers which were constructed in the same format as described in Ref. 4.

In these figures, the p-i-n diode is modelled as a signal photo-current generator, i_{ph}, in parallel with the diode capacitance, C_d, and the associated noise current generators which are the dark-plus-leakage current noise source, i_{dn}, and the quantum noise source, i_{qu}. The feedback resistor[†], R_F, is presented as a noiseless resistor R_F in parallel with its thermal noise source, i_F, and a capacitor C_F which accounts for the stray capacitance across R_F. The input parasitic capacitance of the amplifier is

---

† The name implies a physical resistor which connects the output to the input of an amplifier to create a feedback effect.

- 8 -

represented by C_p. Finally, the front-end transistor is modelled by employing the standard hybrid-π model[4] as shown in Fig. 6 and the subsequent amplification stages are approximated as noiseless amplifiers. This approximation is valid when the first amplification stage (provided by the front-end transistor) is sufficiently large, as more detailed analyses have proven.[1,2,3,4] We will see that this leads to a convenient simplification of the derivation of the receiver equivalent input noise which is presented in Section 2.8.

2.4 - Optical Receiver Operation

The operation of a typical receiver can be explained by the use of Fig. 4 or Fig. 5. The p-i-n detected average signal current, I_{ph}, is related to the average incident optical power, $\overline{P}$, through the quantum efficiency, η, as:

$$I_{ph} = \frac{q}{h\nu} \eta \overline{P} \qquad \text{Ampere} \qquad (1)$$

where q is the electronic charge, h is Planck's constant and ν is the frequency of the incident optical radiation.

This photo-current and the detector noise current flow into the input of the amplifier where they are increased by the addition of the amplifier equivalent input noise current. Then, the total current is transformed into an output voltage by the transimpedance gain of the receiver. Here, this voltage is further processed depending on the

- 9 -

particular application.

2.5 - Detector Noise

As was previously mentioned, detector noise is the summation of shot noise and quantum noise. The spectral density of the quantum noise, can be written as:[2]

$$\frac{d<i^2_{qu}>}{df} = 2qI_{ph} \qquad A^2/Hz \; , \tag{2}$$

where I_{ph} is defined as before and f is the frequency of measurement. Note that this noise term depends upon the signal level and the averaging time is assumed short compared to the signal rate.

The shot noise contribution is given by:

$$\frac{d<i^2_{dn}>}{df} = 2qI_{dn} \qquad A^2/Hz \; , \tag{3}$$

where I_{dn} is the average value of the dark current plus the leakage current.

2.6 - Resistor Noise

Any amplifier has an input loading resistor and/or a feedback resistor and several biasing resistors which are the sources of thermal noise. The thermal noise current generator of a resistor, i_R, is given by:

$$\frac{d \langle i_R^2 \rangle}{df} = \frac{4kT}{R} \qquad A^2/Hz \ , \qquad\qquad (4)$$

where k is Boltzmann's constant and T is the absolute temperature. Note that, by employing Thevenin's theorem Eq. 4 can be rewritten as:

$$\frac{d \langle e_R^2 \rangle}{df} = 4kTR \qquad V^2/Hz \ , \qquad\qquad (5)$$

where e_R is the thermal noise voltage generator of the resistor R.

Within this paper, eq. 4 and eq. 5 are used to represent the thermal noise generators i_F, i_D, i_C and $e_{bb'}$ of the various resistors R_F, R_D, R_C and $r_{bb'}$, respectively.

2.7 - Transistor Noise

The standard hybrid-π noise model is commonly used to model transistors which are employed in optical receivers.[3,4,5,17] This noise model is shown in Fig. 6 where either a FET or a BJT can be represented by filling in the appropriate circuit elements.[4]

2.7.1 - Field Effect Transistor Noise Model

For the FET case, the input noise current generator, i_{in}, is the combination of the gate shot noise, $2qI_{gt}$,[13] and the frequency dependent gate coupling noise, $4kT\Gamma(2\pi f C_T)^2/g_m$,[17] i.e.,

- 11 -

$$\frac{d\langle i_{in}^2 \rangle}{df} = [4kT\Gamma(2\pi f C_T)^2/g_m] + 2qI_{gt} \qquad A^2/Hz \qquad (6)$$

The output noise current generator, i_{out}, is the combination of the channel thermal noise, $4kTg_m P$,[17] and the flicker noise, $4kTg_m \Gamma f_c/f$,[13] i.e,

$$\frac{d\langle i_{out}^2 \rangle}{df} = 4kTg_m P \left[1 + \frac{\Gamma f_c}{Pf} \right] \qquad A^2/Hz . \qquad (7)$$

In these two equations, Γ and P are factors depending on various FET parameters and the gate bias,[18] C_T is the effective input capacitance, g_m is the transconductance, I_{gt} is the average gate leakage current and f_c is the corner frequency at which the flicker noise is equal to the channel noise.

2.7.2 - Bipolar Junction Transistor Noise Model

For the BJT case, i_{in} and i_{out} denote the base and collector shot noise current generators, respectively,[13] i.e.,

$$\frac{d\langle i_{in}^2 \rangle}{df} = 2qI_B \qquad A^2/Hz , \qquad (8)$$

$$\frac{d\langle i_{out}^2 \rangle}{df} = 2qI_C \qquad A^2/Hz , \qquad (9)$$

where I_B and I_C are the average base and collector currents, respectively.

Note that the thermal noise contribution to the current noise generator i_{in} is not listed here. This noise

contribution results from the base spreading resistance $r_{bb'}$. Reader is referred to section 2.8.3 where the derivation of this current noise contribution is given.

2.8 – Receiver Equivalent Input Noise

In theory the total equivalent input noise current of any receiver can be expressed in the form of a frequency-dependent polynominal. In this paper, the total equivalent input noise current of the typical receivers is assumed to be completely generated by the first amplification stage provided by the front-end transistor. This noise current is obtained by summing the total noise current generated at the input of the receiver, $<i_{in}^2>_{total}$, and the total noise current generated at the output of the first amplification stage, $<i_{out}^2>_{total}$, transformed to the input of the receiver. The transformation is made by dividing the total noise generated at the output, $<i_{out}^2>_{total}$, by the current gain, $A_i(f)$, of the front end transistor, i.e.,

$$\frac{d<i_{eq}^2>}{df} = \frac{d<i_{in}^2>_{total}}{df} + \frac{\frac{d<i_{out}^2>_{total}}{df}}{|A_i(f)|^2} , \qquad (10)$$

where $A_i(f)$ can be derived by inspection of Fig. 6:

$$A_i(f) = \frac{I_{out}(f)}{I_{in}(f)} = \frac{Z_1(1-g_m Z_2)}{Z_1 + Z_2} . \qquad (11)$$

For a good transistor, the product $g_m Z_2$ is much greater than

- 13 -

unity over the entire bandwidth of interest. Then $A_i(f)$ is reduced to:

$$A_i(f) = -g_m \left[\frac{z_1 z_2}{z_1 + z_2} \right] = -g_m (z_1 // z_2).$$ (12)

Note that, the method of obtaining the above equivalent input noise current, $<i_{eq}^2>$, implies two assumptions:

1. As mentioned in Section 2.3, all noise sources beyond the first amplification stage can be considered as negligible.

2. All noise sources are uncorrelated.[1,2,4] This assumption is valid by virtue of the following reasons:

    a. Noise which originates from different sources is uncorrelated,[13] e.g., no correlation between the detector shot noise and the front-end transistor shot noise.

    b. In case of the BJT, there is no correlation between the base shot noise and the collector shot noise.[13]

    c. In case of the GaAs FET the correlation of the channel noise and the induced gate noise can be incorporated into the excess channel noise factor Γ as:[17]

$$\dot{P} = P + R(C_{gs}/C_T)^2 - 2Q(C_{gs}/C_T) \ , \tag{13}$$

where P, R and C_T have been defined earlier. C_{gs} is the gate to source capacitance. Q is another factor depending on various FET parameters and the gate bias.[18] For the particular FET in use P=1.24, R=0.30 an Q=-0.42.[17]

2.8.1 - p-i-n FET Receiver Equivalent Input Noise

By inspection of Fig. 4 and the use of Eq. 10, the total equivalent input current noise of the p-i-n FET receiver can be written as:

$$\frac{d<i_{eq}^2>_{p-i-nFET}}{df} = \frac{d}{df}\left[<i_{qu}^2>+<i_{dk}^2>+<i_F^2>+<i_{in}^2>_{FET}\right]$$

$$+ \frac{\frac{d}{df}\left[<i_{out}^2>_{FET}+<i_D^2>\right]}{|A_i(f)|_{FET}^2} \tag{14}$$

where i_D is the thermal noise current of the drain resistor R_D, and $A_i(f)$ is the current gain of the FET, which can be derived by inspection of Fig. 4 and the use of eq. 12:

$$A_i(f)_{FET} = \frac{-g_m R_F}{1+j2\pi f R_F C_T} \ , \tag{15}$$

$$C_T = C_d + C_F + C_p + C_{gs} + C_{gd} \ ,$$

where C_{gd} is the gate to drain capacitance.

Substituting Eq. 2, 3, 4, 6, 7 and 15 into Eq. 11, the total equivalent input current noise spectral density of the p-i-n FET receiver is of the form:

- 15 -

$$\frac{d\langle i_{eq}^2 \rangle_{p-i-nFET}}{df} = af^{-1} + bf^0 + cf^1 + df^2 \qquad (16)$$

where a, b, c and d are the current noise coefficients and their values are:

$$a = 4kT\Gamma f_c/g_m R_F^2 \ ,$$

$$b = 2q(I_{ph}+I_{dn}+I_{gt})+4kT\left[\frac{1}{R_F}+\left[\frac{1}{g_m R_F}\right]^2\left[\frac{1}{R_D}+g_m P\right]\right] \ ,$$

$$c = 16\pi^2 kT\Gamma f_c C_T^2/g_m \ ,$$

$$d = 16kT\left[\frac{\pi C_T}{g_m}\right]^2\left[\frac{1}{R_D} + 2g_m\Gamma\right] \ .$$

From the above equation, the mean square equivalent input current noise of the p-i-n FET receiver can be evaluated as:

$$\langle i_{eq}^2\rangle_{p-i-nFET} = \int_0^\infty W(f)\frac{d\langle i_{eq}^2\rangle_{p-i-nFET}}{df}\ df. \qquad (17)$$

where W(f) is a weighting function dependent upon the receiver's bandshape. This relation will be discussed in more detail in Section 3.9. Here, in the case of W(f) equal to unity, the indefinite integral of Eq. 17 is of the form:

$$\langle i_{eq}^2(f)\rangle_{p-i-nFET} = a\ell nf + bf + \frac{c}{2}f^2 + \frac{d}{3}f^3 \qquad (18)$$

In practice, this integral is evaluated within the receiver's effective noise bandwidth, $B_{eff}=f_H-f_L$, where f_H and f_L, respectively, are the high and low frequency cut-off of the receiver. Usually, $f_H \gg f_L$ so that $B_{eff} \sim f_H$. Using this condition, Eq. 18 becomes

$$\langle i_{eq}^2(B_{eff})\rangle_{p-i-nFET} = a\ \ln\frac{B_{eff}}{f_L} + bB_{eff} + \frac{c}{2}B_{eff}^2 + \frac{d}{3}B_{eff}^3 \quad (19)$$

2.8.2 - Impact of Noise on a Practical p-i-n FET Receiver Design

From the expressions of the noise coefficients a, b, c and d given in eq. 16, a good design of a p-i-n FET receiver implies the following characteristics:

1. The detector should have low dark current and low leakage current (low I_{dn}). Present InGaAsP/InP technology yields very high quality 1.3μm p-i-n detectors. (Typical parameters: $I_{dn}\sim$10 nA, $C_d\sim$0.5 pF, η~85%). So that one can obtain a design which has the contribution of the total detector shot noise to the "b" coefficient one order of magnitude smaller than the contribution of the feed back resistor thermal noise.[1,2,3,4,8] This thermal noise contribution of R_F can be three to four orders of magnitude larger than the total noise contribution from R_D and the FET depending on the particular design. This implies that for a typical p-i-n FET receiver design, the portion of noise which is flat within the receiver bandwidth is dominated by the thermal noise of R_F.

2. As can be seen in eq. 4, the thermal noise current of any resistor is inversely proportional to its resistance. This implies that the values of R_F and R_D

should be chosen as high as possible. Since R_D is
somewhat fixed by the requirement of the biasing
conditions, only R_F exhibits more freedom of choice.
Here, a trade-off exists due to the fact that the
receiver bandwidth decreases with increasing R_F
values.[1,2,3] Usually, one can overcome this effect
by choosing a high value of R_F which produces much
less than the desired bandwidth. Then, an equilizer
is employed at the output of the receiver to restore
the desired bandwidth.[1,2] This method has a limit
since the high frequency noise of succeeding stages of
amplification is no longer negligible when the
equilization ratio becomes large.[1,2]

3. The FET in use should have high figure of merit
    (g_m/C_{gs}). This helps to deemphasize the effect of the
    front-end transistor noise. This can be realized by
    choosing a micro-wave graded FET. Also the FET should
    have low values of Γ, P and f_c. These parameters are
    dependent upon the transistor's technology and can be
    minimized by careful design and fabrication of the
    FET. (Typical parameters: $gm/C_{gs} \sim 50$ GHz, $\Gamma \sim 1.75$,
    $P \sim 1.24$, $f_c \sim 25$ MHz).

Note that, from the compositions of the noise
coefficients c and d of eq. 16, it looks like the effective
input capacitance, C_T, is causing noise. However, this

- 18 -

noise is not generated by the capacitor which is a noiseless element, but rather results from the action of the current gain, $A_i(f)$, upon the transistor's output noise generators. It can be seen in eq. 15 that $A_i(f)$ decreases with increasing frequency. By virtue of eq. 10, the contribution of the total output noise of the front-end transistor to the equivalent input noise of the receiver is proportional to frequency. This effect can be optimized by choosing low capacitance circuit elements to use at the input of the receiver.

2.8.3 - p-i-n BJT Receiver Equivalent Input Noise

In a similar manner to that used for the p-i-n FET receiver, the expression for the equivalent input noise current of the p-i-n BJT receiver can be formulated by inspection of Fig. 5 and the use of Eq. 10, i.e.,

$$\frac{d\langle i_{eq}^2 \rangle_{p-i-nBJT}}{df} = \frac{d}{df}\left[\langle i_{qu}^2 \rangle + \langle i_{dn}^2 \rangle + \langle i_F^2 \rangle + \langle i_b^2 \rangle + \langle i_{in}^2 \rangle_{BJT}\right]$$

$$+ \frac{\frac{d}{df}\left[\langle i_{out}^2 \rangle_{BJT} + \langle i_C^2 \rangle\right]}{|A_i(f)|^2_{BJT}} \qquad (20)$$

where i_C is the noise contribution of R_C, and $i_{b'}$ is the noise contribution of the spreading resistance, r_{bb}', which can be derived as follows:

$$\frac{d<i^2_{b'}>}{df} = \frac{\frac{d}{df}<e^2_{bb'}>}{|R'|^2} \qquad (21)$$

where

$$\frac{d}{df}<e^2_{bb'}> = 4kTr_{bb'} \quad,$$

$$R' = \frac{R_F}{1+j2\pi fR_FC'} \quad,$$

$$C' = C_d+C_F+C_p \quad.$$

$A_i(f)$, in this case is the short circuit current gain of the front end BJT including the loading effect, which can be written as:

$$A_i(f)_{BJT} = \frac{-g_mR''}{1+j2\pi fR''C_T} \qquad (22)$$

where

$$R'' = R_F//r_{b'e}$$

$$C_T = C_d+C_F+C_p+C_{b'e}+C_{b'c}$$

In the above equation, the loading effect of $r_{bb'}$ is neglected since $r_{bb'}<<r_{b'e}$. Also $C_{b'e}$ and $C_{b'c}$ are respectively the shunt and series capacitances of the BJT.

Substituting Eq. 2, 3, 4, 8, 9, 21 and 22 into Eq. 20, the total equivalent input current noise spectral density of the p-i-n BJT receiver is of the form:

$$\frac{d<i^2_{eq}>_{p-i-nBJT}}{df} = a + bf^2 \qquad (23)$$

where

$$a = 2q \left[I_{qu} + I_{dn} + I_B + \frac{I_C}{(g_m R'')^2} \right] + 4kT \left[\frac{1}{R_F} + \frac{r_{bb}'}{R_F^2} + \frac{1}{R_C (g_m R'')^2} \right]$$

$$b = 16\pi^2 kT \left[r_{bb}' C'^2 + \frac{1}{R_C} \left[\frac{C_T}{g_m} \right]^2 \right] + 8q I_C \left[\frac{\pi C_T}{g_m} \right]^2 .$$

From Eq. 22, the mean square equivalent input noise current of the p-i-n BJT receiver as a function of the effective noise bandwidth, $B_{eff} = f_H - f_L$ where $B_{eff} \sim f_H$ since $f_H \gg f_L$, can be written as:

$$<i_{eq}^2 (B_{eff})>_{p-i-nBJT} = aB_{eff} + \frac{b}{3}B_{eff}^3 \qquad (24)$$

2.8.4 - Impact of Noise on a Practical p-i-n BJT Receiver Design

As a benefit of the well known Si-BJT technology, a good BJT does not exhibit flicker noise above a few KHz. Normally, only shot noise which results from the biasing currents I_B and I_C, and the thermal noise which results from the base spreading resistance, r_{bb}', are important. This implies the absence of the two noise terms resulting from the flicker noise in eq. 24 compared to eq. 19. Since the detector's effect on noise in both eq. 16 and eq. 23 is the same, the discussion of the detector's effect on noise given in the previous section is applicable here. However, due to the large amount of shot noise resulting from I_B, the shot noise term of the noise coefficient "a" is now comparable in magnitude to the thermal noise term resulting from the various resistances R_F, r_{bb}' and R_C. Within this thermal

noise term, the noise resulting from R_F still dominates the others in a typical design. This implies that for a typical p-i-n BJT receiver, the portion of noise which is flat within the receiver bandwidth is dominated both by the thermal noise of R_F and the shot noise of I_B.

One of the special noise features of a BJT is the significant noise contribution of the spreading resistance $r_{bb'}$ to the noise coefficient "b". (Typically $r_{bb'} \leq 100\Omega$). In a typical receiver, the thermal noise due to $r_{bb'}$ can be of the same order of magnitude as the shot noise due to I_C.

The noise effect of C_T has been previously discussed: as a rule of thumb one should keep all capacitances which are associated with the input of the receiver as low as possible.

2.9 - Bit Error Rates for Digital Transmission

We proceed next to the prediction of receiver performance based upon the derivation of the equivalent input noise current spectral density for both p-i-n BJT and p-i-n FET optical receivers. By comparing the rms equivalent input noise current, $<i_{eq}^2>^{1/2}$, to the rms photo-induced signal current, $<i_{ph}^2>^{1/2}$, the sensitivity of an optical receiver can be predicted.

The major application of optical receivers is for digital transmission system, where the sensitivity of a

- 22 -

receiver is defined as the minimum detected optical power, $\eta\bar{P}$, which must reach the receiver in order to achieve a given bit error rate (BER). Personick[2] has shown that for a practical digital system which operates at 10^{-9} BER (one error per billion bits of digital transmission), the signal to noise ratio (S/N) is equal to 6. Note that, in deriving the above S/N ratio, Personick has assumed that Gaussian statistics governed all receiver noise sources. This is not so, since the statistics of the optical signal and the p-i-n detector noise are characterized by Poisson statistics.[13] However, it has been shown that the results obtained by assuming all statistics are Gaussian yield predicting in close agreement with the exact calculation done by digital computation, especially for the range of parameters encountered in optical fiber systems.[19]

As an immediate application for the receivers which are considered in this paper, the receiver sensitivities can be formulated by the use of Eq. 1, i.e.,

$$\eta\bar{P}_{10^{-9}BER} = 10 \log (5.7 \times 10^3 < i_{eq}^2 >^{1/2}) \text{ dBm}, \qquad (25)$$

where $< i_{eq} >^{1/2}$ is given in Ampere and $(h\nu/q)=0.95$ W/A for $\lambda=1.3\mu m$ has been utilized. Note that, the above equation demonstrates that the sensitivity of any practical receiver can be derived solely from the value of the equivalent input noise current which can be determined from the knowledge of the equivalent input noise spectral density of the receiver

plus the overall system band shape.

SECTION 3. MEASUREMENT METHOD

The purpose of the experiment is to determine accurately the coefficients of the equivalent input noise current polynomial. Since these coefficients depend directly on the receiver circuit parameters and can be derived by theoretical computation, a direct and detailed comparison between theory and experiment becomes possible.

3.1 - Experimental Apparatus

The experimental apparatus is shown in Fig. 7. The controller, plotter, signal generator, post amplifier and spectrum analyzer are all commercial products (Hewlett-Packard 9825A, 9872A, 8662A, 8447D and 8568A, respectively.). The 1.3μm analog laser transmitter and the experimental 1.3μm receivers (p-i-n FET and p-i-n BJT) were built especially for this experiment, using modifications of the designs by P. Swarup,[9] K. Ogawa[8] and R. Paski[10] of Bell Labs, respectively.

3.2 - Equivalent Circuit and Its Operation

The equivalent circuit for this apparatus, as seen by the spectrum analyzer, is shown in Fig. 8. In operation, the controller is programmed to command the signal generator to sine-wave modulate the transmitter at a series of

frequencies, and at each frequency the controller also commands the analyzer to track the fundamental frequency of the photo-generated and amplified signal with a resolution bandwidth much smaller than the receiver bandwidth (1 KHz to 1.2 MHz for the p-i-n FET, and 10 KHz to 300 MHz for the p-i-n BJT), so that as the center frequency of the analyzer is swept over the receiver bandwidth, the output electrical power spectrum, $P_{out}(f)$, is measured and stored on tape for later manipulation and plotting.

From the measured values of the output electrical power and the input optical power, the value of the receiver equivalent input noise current spectrum, $<i_{eq}^2(f)>$, can be determined.

3.3 - Output Noise Measurement

The relationship between $P_{out}(f)$ and $<i_{eq}^2(f)>$ can be theoretically explained by inspection of Fig. 8:

$$<v_{out}^2(f)> = <i_{total}^2(f)>|R(f)|^2|G(f)|^2 , \qquad (26)$$

where $G(f)$ is the post-amplifier voltage gain spectrum, and $<i_{total}^2(f)>$ is the receiver total mean square input current spectrum due to both signal and noise and is defined by:

$$<i_{total}^2(f)> = <i_{ph}^2(f)>+<i_{eq}^2(f)> \qquad (27)$$

Note that, in Eq. 26 the assumptions of $<i_{total}^2(f)>|R(f)|^2 >> <e_{pa}^2(f)>$ (post-amplifier equivalent input voltage noise) and $<v_{out}^2(f)> >> <e_{sa}^2(f)>$ (spectrum

- 25 -

analyzer equivalent input voltage noise), are implicit. (In practice these assumptions turn out to be well justified. In principle $<e_{pa}^2(f)>$ and $<e_{sa}^2(f)>$ can be normalized out of the measurement, if extreme accuracy is desired.)

From Eq. 27, when $<i_{ph}^2(f)>=0$ (no optical power input to the receiver), Eq. 26 becomes:

$$<v_1^2(f)> = <i_{eq}^2(f)>|R(f)|^2|G(f)|^2 \qquad (28)$$

This voltage noise spectrum seen by the analyzer is expressed as a power spectrum:

$$P_1(f) = 10\log\left[\frac{<v_1^2(f)>}{50\Omega}\times10^3\right] \qquad \text{dBm} \qquad (29)$$

Note that, in order to determine $<i_{eq}^2(f)>$ from Eq. 28, $|R(f)|^2$ and $|G(f)|^2$ have to be known.

3.4 - Receiver Transimpedance Gain Measurement

The measurement procedure to determine $|R(f)|^2$ is readily available from Eq. 26 and Eq. 27. Note that, in Eq. 27, when $<i_{ph}^2(f)> >> <i_{eq}^2(f)>$, Eq. 26 becomes:

$$<v_2^2(f)> = <i_{ph}^2(f)>|R(f)|^2|G(f)|^2 , \qquad (30)$$

and the associated power spectrum, as measured by the analyzer, is:

$$P_2(f) = 10 \, \log \left[\frac{<v_2^2(f)>}{50\Omega} \times 10^3 \right] \qquad \text{dBm} \, . \qquad (31)$$

To be free of $<i_{ph}^2(f)>$ in Eq. 30, a p-i-n diode (reference diode) similar to the one in use in the receiver is terminated with a resistive output impedance, R_L, and is used to replace the receiver in Fig. 7 (Note that, $1/2\pi R_L C_d$ >> f_H, so that the apparatus used for normalization has a response which is independent of frequency over the bandwidth of interest). Graphically, the change of Fig. 7 is shown in Fig. 9 and its equivalent circuit diagram as seen by the analyzer is shown in Fig. 10.

In order to keep the noise of the post-amplifier and the spectrum analyzer negligible, the photo-current is increased by a factor of k to compensate for the low value of R_L compared to $|R(f)|$. By inspection of Fig. 10, when $k^2 <i_{ph}^2(f)>$ >> $<i_{eq}^2(f)>$, the factor k can be written as:

$$k = \frac{I_{ph \, p-i-n}}{I_{ph \, receiver}} \, , \qquad (31)$$

where $I_{ph \, p-i-n}$ is the average photo-current generated by the reference diode and $I_{ph \, receiver}$ is the average photo-current generated by the diode in the receiver. In this case, the mean square output voltage, $<v_3^2(f)>$, can be expressed as:

$$<v_3^2(f)> = k^2 <i_{ph}^2(f)> R_L^2 |G(f)|^2 \, , \qquad (33)$$

and the analyzer measures $<v_3^2(f)>$ as:

- 27 -

$$P_3(f) = 10 \log \left[\frac{<v_3^2(f)>}{50\Omega} \times 10^3 \right] \quad \text{dBm .} \quad (34)$$

By utilizing Eq. 30 through Eq. 34, $|R(f)|^2$ can be expressed as:

$$|R(f)|^2 = k^2 R_L^2 \frac{<v_2^2(f)>}{<v_3^2(f)>} = k^2 R_L^2 \times 10^{0.1[P_2(f)-P_3(f)]} \quad (35)$$

3.5 - Post-amplifier Gain Measurement

To measure $|G(f)|^2$, the apparatus of Fig. 11 is employed. First the signal generator is set at $v_4(f)$ where $<v_4^2(f)> \gg <e_{sa}^2(f)>$. The analyzer measures $v_4(f)$ and expresses it as a power spectrum:

$$P_4(f) = 10 \log \left[\frac{<v_4^2(f)>}{50\Omega} \times 10^3 \right] \text{dBm.} \quad (36)$$

Then $P_4(f)$ is used as the input to the post-amplifier, and at the output of the post-amplifier another power spectrum is measured:

$$P_5(f) = 10 \log \left[\frac{<v_5^2(f)>}{50\Omega} \times 10^3 \right] \text{dBm .} \quad (37)$$

Since v_4 and v_5 are the input and output voltage of the post-amplifier, respectively $|G(f)|^2$ can be written as:

$$|G(f)|^2 = \frac{\langle v_5^2(f) \rangle}{\langle v_4^2(f) \rangle} = 10^{0.1[P_5(f) - P_4(f)]} \qquad (38)$$

3.6 - Receiver Equivalent Input Noise Transformation

Finally, the equivalent input mean square noise current spectrum of the receiver under examination, $\langle i_{eq}^2(f) \rangle$, can be determined by substituting Eq. 29, 35, 38 into Eq. 28 and rearranging as below:

$$\langle i_{eq}^2(f) \rangle = \frac{\langle v_1^2(f) \rangle}{|R(f)|^2 |G(f)|^2}$$

$$= \frac{5 \times 10^{-2}}{k^2 R_L^2} \times 10^{0.1[P_1(f) - P_2(f) + P_3(f) + P_4(f) - P_5(f)]} \qquad (39)$$

Note that, by normalizing $\langle v_1^2(f) \rangle$ or $P_1(f)$ to 1 Hz noise bandwidth and assuming:

$$\frac{d \langle i_{eq}^2(f) \rangle}{df} \equiv \frac{\langle i_{eq}^2(f) \rangle}{1 \text{ Hz}},$$

eq. 39 can be used to generate the equivalent input noise current spectral density of the receiver under measurement, i.e.,

$$\frac{d \langle i_{eq}^2(f) \rangle}{df} = \frac{\langle v_1^2(f) \rangle_{1Hz}}{|R(f)|^2 |G(f)|^2|}$$

$$= \frac{5 \times 10^{-2}}{k^2 R_L^2} \times 10^{0.1[P_1(f)_{1Hz} - P_2(f) + P_3(f) + P_4(f) - P_5(f)]} \qquad (40)$$

Practically, this measurement employs a technique where $|R(f)|^2$ and $|G(f)|^2$ are normalized by determining ratios of experimental quantities. Thus the accuracy with which $<i_{eq}^2(f)>$ can be measured is determined primarily by the accuracy of the spectrum analyzer in measuring $P_1(f)$. With the self-calibration feature of the HP-8568A spectrum analyzer the accuracy of $P_1(f)$ can be made to be ± 0.4 dB.

3.7 - Measurement Results

The equivalent circuit diagrams which explain the technique used to measure $<i_{eq}^2(f)>$ for the p-i-n FET and p-i-n BJT receivers are given in Fig. 12[†] and Fig. 13, respectively. Fig. 14 and Fig. 15 show the results of these measurements of the equivalent input noise current spectral densities. Note that the theoretical curves are plotted by using Eq. 16 for the p-i-n FET receiver and Eq. 23 for the p-i-n BJT receiver. These theoretical curves were generated by adjusting the circuit's parameters slightly from their

---

[†] Note that, in order to show the effect of the flicker noise upon the p-i-n FET receiver equivalent input noise spectral density, it is better to start the measurements at frequency as low as the experimental apparatus would allow. In the apparatus employed in this experiment, the HP-8662A signal generator has a low frequency limit (f_L) value of 10 KHz, whereas the HP-8447D amplifier has a f_L value of 100 KHz. Therefore, it is convenient to replace the HP-8447D amplifier by two Avantek amplifiers (model UAA) connected in cascade, which have f_L value of 5 KHz, so that the measurements can start at a frequency of 10 KHz.

nominal design values in order to obtain a good agreement with experiment. Since only slight adjustment was needed to make theory and experiment agree, we were justified in our assumption that only the front-end transistor contributes significantly to the amplifier's equivalent input noise. Values for these parameters can be found in Table 1 for the p-i-n FET and Table 2 for the p-i-n BJT. These parameters are discussed further in Section 4 of this paper.

Also, in order to effectively compare the measured results against the theoretical predictions, it is necessary to obtain the measured noise coefficients. This is done by employing the least-square-fit method. The results of the measured noise coefficients are given in Table 1 and Table 2 for the p-i-n FET receiver and the p-i-n BJT receiver respectively. The least-square-fit curves are plotted in the same graphs together with the corresponding measured data points and the theoretical curves. These are shown in Fig. 14 and Fig. 15 for the respective receivers.

3.8 - Least Square Fit

The least-square-fit method[7] was employed to determine the measured noise coefficients of the receiver equivalent input noise current spectral densities. Since the results of this process are the smooth functions, it also helps to simplify the calculations of the total noise power per bandwidth. This was used in conjunction with eq.

25 to determine the respective receiver sensitivities. More detail of this evaluation process is given in the next section.

The least-square-fit method minimizes the sums of squares of the deviation of the scattered data point about the expected theoretical form of $<i^2_{eq}(f)>$. Mathematically expressed, the fitting process is the minimization of

$$Q= \sum_{i=1}^{n} \left[<i^2_{eq}(f)>_i - <i^2_{eq}(f_i)> \right]^2, \qquad (41)$$

where Q is defined as a measure of the overall disagreement between the observed values and the predicted theoretical values, n is the number of data points, $<i^2_{eq}(f)>_i$ is the measured value of $<i^2_{eq}(f)>$ at the $i\underline{th}$ data point and $<i^2_{eq}(f_i)>$ is the expected theoretical value of $<i^2_{eq}(f)>$ evaluated at the $i\underline{th}$ frequency of measurement. The mathematical detail of this technique is given in the appendix.

3.9 - Receiver Performance Evaluation

An indication of the performance of the receivers under examination is given in Fig. 16 and Fig. 17 which are the plots of receiver sensitivity $(\eta\bar{P})$ as a function of transmission bit rate (B) for the p-i-n FET and p-i-n BJT receivers, respectively. The data points with error bars associated were obtained from actual system measurements on

similar receivers.[10,11,12] The single data points were
measured using the actual receivers characterized in this
paper. These data points obtained from actual bit-error-
rate measurements agree well with each of the two curves
shown. The first curve was generated by integrating the
polynomials obtained from a least-square-fit of the measured
noise. The second curve was obtained from the theoretical
circuit parameters used for good agreement with the measured
noise.

In plotting these curves, it is necessary to define the
weighting function, W(f). Physically W(f) is the system
transfer function, and in a practical fiber communication
system it usually is the product of series of transfer
functions determined by the receiver and the wave-shaping
circuit, i.e.,

$$W(f) = \frac{R(f)\ G(f)\ E(f)\ F(f)}{R_oG_oE_oF_o} , \qquad (42)$$

where the product R(f) G(f) is the receiver's transfer
function and the product E(f) F(f) is the wave-shaping
circuit's transfer function resulting from the equalizer and
filter responses, respectively. Note that, $R_oG_oE_oF_o$ is the
product of the midband values of the associated transfer
functions.

In this paper, for simplicity, W(f) is assumed to be an
ideal rectangular low-pass filter, i.e.,

$$W(f) = \begin{array}{ll} 1 & 0 \le f \le B_{eff} \\ 0 & \text{otherwise} \end{array} \qquad (43)$$

where B_{eff} is equal to half of transmission bit rate[†] i.e.,
$B_{eff} = 0.5\ B$.

Then the evaluation of $\langle i_{eq}^2(B) \rangle$ can be formulated by
the use of eq. 17, i.e.,

$$\langle i_{eq}^2(B) \rangle = \int_0^{.5B} \frac{d\langle i_{eq}^2(f) \rangle}{df}\ df \ . \qquad (44)$$

The effect of the weighting function is further explained
graphically in Fig. 18, where we see that compared to the
ideal rectangular response a practical system response de-
emphasizes the noise for $f < 0.5B$ and overemphasizes the noise
for $0.5B < f < B_{eff}$.

Note that, if all system components were available for
evaluation, rather than just the receiver, then $\langle i_{eq}^2(B) \rangle$
could be accurately measured including the effect of the
actual system response, $W(f)$. Here, for the case of the
ideal filter, Fig. 16 and Fig. 17 are generated by utilizing
eq. 25.

[†] Nyquist rate[15]

SECTION 4. DISCUSSION

Some useful observations about the results of these measurements can be drawn by inspection of table 1, 2 and Fig. 14 through Fig. 17.

From table 2, Fig. 15 and Fig. 17, it is seen that results of measurements performed on the p-i-n BJT receiver agree well with theory if the effective noise capacitance value (C_T) of 3.4 pF and the transconductance value (g_m) of 50.6 mS are used instead of the values of 3.13 pF and 58.5 mS which were originally used in the circuit design model. It was not possible to directly measure all of the circuit's parameters, but the values used did fall within the range measured on similar circuit elements, (as shown in Table 2).

From table 1, Fig. 14 and Fig. 16 results of measurements performed on the p-i-n FET receiver indicate little discrepancy from the theoretical expectation of the receiver's sensitivity if the flicker noise corner (f_c) of 50 MHz, and the shunt capacitance (C_{gs}) of 0.6 pF are used instead of the values of 25 MHz, and 0.5 pF which were used in the circuit design model. Here also, the parameters lie within the range of values measured on similar devices.

From table 1, it is seen that whereas all other noise coefficients are close to their theoretical values, the flicker noise coefficient is almost triple its theoretical

value. Fig. 14 which is a log-log plot of the equivalent

input noise spectral density of the p-i-n FET receiver

clarifies this effect. However, this discrepancy has little

penalty on the total integrated noise[†] which is directly

proportional to the receiver's sensitivity.[††] From the two

curves in Fig. 16 it is seen that for operating bit rates of

1 Mb/s$\leq$B$\leq$10 Mb/s the discrepancy in receiver's sensitivity

due to this flicker noise is at most 0.3 dB. For bit rates

of more than 10 Mb/s where this particular receiver is

designed for use, the receiver's sensitivity does not suffer

a significant loss from this discrepancy. From this result,

it is suggested that for a p-i-n FET receiver which is

designed to operate at lower bit rates (B$\leq$1 Mb/s), the

flicker noise may have to be characterized more accurately.

The discrepancies between the data points and the

curves in Figures 16 and 17 must be due to causes other than

the receiver's equivalent input noise. Possible sources of

this degradation from ideal performance include: non-ideal

response function W(f) for the linear channel,[†††] excess

[†] See Eq. 17.

[††] See eq. 25.

[†††] The linear channel refers to the additional gain and
wave-shaping circuit. Its function is to provide enough
gain for the particular application and to reshape the
distorted signal which is received after a long distance
of transmission.

noise in the linear channel, non-ideal optical pulses from the laser transmitters (noise, intersymbol interference, jitter), and non-ideal response in the decision circuit.[†] The fact that there is a larger discrepancy for the p-i-n FET receiver than for the p-i-n BJT receiver is probably due to the need for an equalizer between the p-i-n FET receiver and the linear channel which tends to emphasize the noise from the linear channel.[2]

Finally, it has been shown that with a little adjustment in the circuit parameters, the theoretical noise models of the receivers under examination can be used to reflect very accurately the performances of the practical receivers.

SECTION 5. CONCLUSION

Within the body of this paper, an analysis of noise in p-i-n FET and p-i-n BJT optical receivers has been given. By applying straight-forward circuit analysis, it has been shown theoretically that the receiver performance can be evaluated solely in terms of the equivalent input noise current, most of which originates in the front-end

---

[†] For a digital system an additional function, that of a decision circuit, would be required. Its function is to compare the signal from the linear channel against a threshold level which is set higher than the noise level to properly produce an '1' or a '0' at the output.

transistor in typical receivers.

Experimentally, two typical receivers have been constructed and evaluated. Good agreement between theoretically and experimentally derived receiver equivalent input noise was obtained.

In the literature, several authors[1,3,4,5] have theoretically derived the equivalent input noise current for an arbitrary optical receiver. Also there is one paper[20] in which the equivalent input noise current spectrum of a receiver was measured by a method which was less accurate than the one presented here and which was not automated. The automated measurement technique presented here is unique by virtue of its accuracy and fast measurement results. This method will be employed to economically manufacture high quality optical receivers.[16]

REFERENCES

[1] Personick, S. D., "Receiver Design for Digital Fiber Optic Communication Systems," Bell System Technical Journal 2, pp. 843-886, 1973.

[2] Personick, S. D. and Smith, R. G., "Receiver Design for Optical Fiber Communication Systems," Topics in Applied Physics. Vol. 39, pp. 89-160, 1980.

[3] Hullett, J. L. and Muoi, T. V., "A Feedback Receiver Amplifier for Optical Transmission Systems," IEEE Trans. Commun. COM-24, pp. 1180-1185, 1976.

[4] Hullett, J. L. and Moustakas, S., "Noise Modeling For Broad Band Amplifier Design," IEEE Proc. Vol. 128 No. 2, pp. 67-76, 1981.

[5] Schlachetzki, A. and Aytac, S., "Analysis of an Optical Receiver Front-end for Integration on InGaAsP/InP", Fiber and Integrated Optics, Vol. 3, No. 4, pp. 363-382, 1981.

[6] Melchior, H., "Demodulation and Photo-detection Techniques," Laser Handbook, Vol. 1, edited by Arecchi, F. T. and Schulz-Dubois, E.O., p. 725, 1972.

[7] Davies, O. L., "Statistical Methods in Research on Production," III Edition, Hafner Publishing Company, pp. 208-272, 1957.

[8] Ogawa, K. and Chinock, E. L. "GaAs FET Transimpedance Front End Design for a Wideband Optical Receiver," Electronics Letters, 15, pp 650-652, 1979.

[9] Swarup, P. B., private communication.

[10] Paski, R. M., private communication.

[11] Owen, B., private communication.

[12] Ogawa, K., private communication.

[13] Van Der Zeil, A., "Noise: Sources, Characterization, Measurement," Prentice-Hall, 1970.

[14] Lee, T. P., and Li, T., "Photodetectors," Optical Fiber Telecommunication, edited by Miller and Chynoweth, Academic Press, pp 593-626, 1979.

[15]   Schwartz, M., "Information Transmission, Modulation, and Noise," III Edition, McGraw-Hill, pp 176-188, 1980.

[16]   Snodgrass, M. L., private communication.

[17]   Ogawa, K., "Noise caused by GaAs MESFETs in Optical Receivers," Bell System Technical Journal, Vol. 60, No. 6, July-August 1981, pp 923-928.

[18]   Baechtold, W., "Noise Behavior of Schotty Barrier Gate Field-Effect Transistors at Microwave Frequencies," IEEE Trans. Electron Device, ED-18, No. 2, Feb. 1971, pp 97-104.

[19]   Personick, S. D., Balaban, P., Bobsin, J. H., Kumar, P. K., IEEE Trans. C-25, pp 541, 1977.

[20]   Smith, R. G., Brackett, C. A., and Reinhold, H. W., "Optical Detector Package," Bell System Technical Journal, Vol. 57, No. 6, July-August 1978, pp 1809-1821.

By substituting Eq. 16 for $<i^2_{eq}(f_i)>$ in Eq. 41. The least square deviation between measured and theoretical values for $<i^2_{eq}(f)>_{p-i-n \; FET}$ can be formulated

$$Q_{p-i-n \; FET} = \sum_{i=1}^{n}\left[<i^2_{eq}(f)>_i - \left[\frac{a}{f_i}+b+cf_i+df_i^2\right]\right]^2$$

The minimization process can be done by employing the method of differential calculus, where the partial derivatives of the above eq. with respect to a, b, c and d are each equated to zero giving a set of four simultaneous equation for the desired values of the coefficients a, b, c and d and are obtained as below:

$$\frac{\delta Q_{p-i-nFET}}{\delta a} = 2\sum_{i=1}^{n}\left[<i^2_{eq}(f)>_i - \left[\frac{a}{f_i}+b+cf_i+df_i^2\right]\right]\left[-\frac{1}{f_i}\right] = 0$$

$$\frac{\delta Q_{p-i-nFET}}{\delta b} = 2\sum_{i=1}^{n}\left[<i^2_{eq}(f)>_i - \left[\frac{a}{f_i}+b+cf_i+df_i^2\right]\right](-1) = 0$$

$$\frac{\delta Q_{p-i-nFET}}{\delta c} = 2\sum_{i=1}^{n}\left[<i^2_{eq}(f)>_i - \left[\frac{a}{f_i}+b+cf_i+df_i^2\right]\right](-f_i) = 0$$

$$\frac{\delta Q_{p-i-nFET}}{\delta d} = 2\sum_{i=1}^{n}\left[<i^2_{eq}(f)>_i - \left[\frac{a}{f_i}+b+cf_i+df_i^2\right]\right]\left[-f_i^2\right] = 0$$

Rearranging:

$$a\sum_{i=1}^{n}\frac{1}{f_i^2} + b\sum_{i=1}^{n}\frac{1}{f_i} + cn + d\sum_{i=1}^{n}f_i = \sum_{i=1}^{n}\frac{<i^2_{eq}(f)>_i}{f_i}$$

$$a\sum_{i=1}^{n}\frac{1}{f_i} + bn + c\sum_{i=1}^{n}f_i + d\sum_{i=1}^{n}f_i^2 = \sum_{i=1}^{n}<i^2_{eq}(f)>_i$$

$$an + b\sum_{i=1}^{n}f_i + c\sum_{i=1}^{n}f_i^2 + d\sum_{i=1}^{n}f_i^3 = \sum_{i=1}^{n}<i^2_{eq}(f)>_if_i$$

$$a\sum_{i=1}^{n}f_i + b\sum_{i=1}^{n}f_i^2 + c\sum_{i=1}^{n}f_i^3 + d\sum_{i=1}^{n}f_i^4 = \sum_{i=1}^{n}<i^2_{eq}(f)>_if_i^2$$

Using matrix algebra notation, the above set of equations can be rewritten as:

$$aa_{11} + ba_{12} + ca_{13} + da_{14} = b_1$$

$$aa_{21} + ba_{22} + ca_{23} + da_{24} = b_2$$

$$aa_{31} + ba_{32} + ca_{33} + da_{34} = b_3$$

$$aa_{41} + bas_{42} + ca_{43} + da_{44} = b_4$$

where

$$a_{11} = \sum_{i=1}^{n} \frac{1}{f_i^2}$$

$$a_{12} = a_{21} = \sum_{i=1}^{n} \frac{1}{f_i} \, ,$$

$$a_{13} = a_{22} = a_{31} = n \, ,$$

$$a_{14} = a_{23} = a_{32} = \sum_{i=1}^{n} f_i \, ,$$

$$a_{24} = a_{33} = a_{42} = \sum_{i=1}^{n} f_i^2 \, ,$$

$$a_{34} = a_{43} = \sum_{i=1}^{n} f_i^3 \, ,$$

$$a_{44} = \sum_{i=1}^{n} \frac{<i_{eq}^2(f)>_i}{f_i}$$

$$b_1 = \sum_{i=1}^{n} f_i^4 \, ,$$

$$b_2 = \sum_{i=1}^{n} <i_{eq}^2(f)>_i$$

$$b_3 = \sum_{i=1}^{n} <i_{eq}^2(f)>_i f_i$$

$$b_4 = \sum_{i=1}^{n} <i_{eq}^2(f)>_i f_i^2$$

In order for this system of 4 simultaneous equations to have solutions, its determinant cannot vanish, i.e.,

$$|D| = \begin{vmatrix} a_{11} & a_{12} & a_{13} & a_{14} \\ a_{21} & a_{22} & a_{23} & a_{24} \\ a_{31} & a_{32} & a_{33} & a_{34} \\ a_{41} & a_{42} & a_{43} & a_{44} \end{vmatrix} \neq 0$$

Then the solutions for a, b, c and d can be found as

follows:

$$a = \frac{\begin{vmatrix} b_1 & a_{12} & a_{13} & a_{14} \\ b_2 & a_{22} & a_{23} & a_{24} \\ b_3 & a_{32} & a_{33} & a_{34} \\ b_4 & a_{42} & a_{43} & a_{44} \end{vmatrix}}{|D|} \quad ,$$

$$b = \frac{\begin{vmatrix} a_{11} & b_1 & a_{13} & a_{14} \\ a_{21} & b_2 & a_{23} & a_{24} \\ a_{31} & b_3 & a_{33} & a_{34} \\ a_{41} & b_4 & a_{43} & a_{44} \end{vmatrix}}{|D|} \quad ,$$

$$c = \frac{\begin{vmatrix} a_{11} & a_{12} & b_1 & a_{14} \\ a_{21} & a_{22} & b_2 & a_{24} \\ a_{31} & a_{32} & b_3 & a_{34} \\ a_{41} & a_{42} & b_4 & a_{44} \end{vmatrix}}{|D|} \quad ,$$

$$d = \frac{\begin{vmatrix} a_{11} & a_{12} & a_{13} & b_1 \\ a_{21} & a_{22} & a_{23} & b_2 \\ a_{31} & a_{32} & a_{33} & b_3 \\ a_{41} & a_{42} & a_{43} & b_4 \end{vmatrix}}{|D|}$$

Similarly, for the $<i^2_{eq}(f)>_{p-i-nBJT}$ case, Eq. 23 is substituted into Eq. 41 to give:

$$Q_{p-i-nBJT} = \sum_{i=1}^{n}\left[<i^2_{eq}(f)>_i - \left[a+bf^2_i\right]\right]^2$$

The partial derivatives with respect to a and b are:

$$\frac{\delta Q_{p-i-nBJT}}{\delta a} = 2\sum_{i=1}^{n}\left[<i^2_{eq}(f)>_i - \left[a+bf^2_i\right]\right](-1) = 0$$

$$\frac{\delta Q_{p-i-nBJT}}{\delta b} = 2\sum_{i=1}^{n}\left[<i^2_{eq}(f)>_i - \left[a+bf^2_i\right]\right](-f^2_i) = 0$$

Rearranging and using matrix algebra notations, i.e.,

$$aa_{11} + ba_{12} = b_1$$

$$aa_{21} + ba_{22} = b_2$$

where

- 43 -

$$a_{11} = n$$

$$a_{12} = a_{21} = \sum_{i=1}^{n} f_i^2$$

$$a_{22} = \sum_{i=1}^{n} f_i^4$$

$$b_1 = \sum_{i=1}^{n} <i_{eq}^2(f)>_i$$

$$b_2 = \sum_{i=1}^{n} <i_{eq}^2(f)>_i f_i^2$$

Solving for a and b:

$$|D| = \begin{vmatrix} a_{11} & a_{12} \\ a_{21} & a_{22} \end{vmatrix} \neq 0 \; ,$$

$$a = \left| \frac{\begin{vmatrix} b_1 & a_{12} \\ b_2 & a_{22} \end{vmatrix}}{|D|} \right.$$

$$b = \left| \frac{\begin{vmatrix} a_{11} & b_1 \\ a_{21} & b_2 \end{vmatrix}}{|D|} \right.$$

BIOGRAPHICAL SKETCH

THANH VAN NGUYEN

Born February 24, 1955 in Vietnam. Parents names Thi Thi (Ly) and Thom Van Nguyen. Immigrated to United States in August, 1975 and nationalized in November, 1981. Married Claudeen Fay (Gernert) in November, 1981. One child, Justin Van Nguyen (1 year old).

GRADUATE

Chau Van Tiep High School, Vietnam, 1973

National Teacher College, Vietnam, Associate Degree in Elementary Education, 1975.

Harrisburg Area Community College, Harrisburg, PA, Associate Degree in Electro-Mechanical Engineering, 1978.

Pennsylvania State University (Capitol Campus), Middletown, PA, Bachelor of Technology Degree in Electrical Design Engineering (Honor), 1980.

EXPERIENCE

Employed by Bell Laboratories of Allentown, PA., as a Senior Technical Associate. Past assignments have been related to the development of the 1.3μm optical receivers for long-haul applications. Present assignment is related to the development of the 1.5μm single frequency laser transmitters.
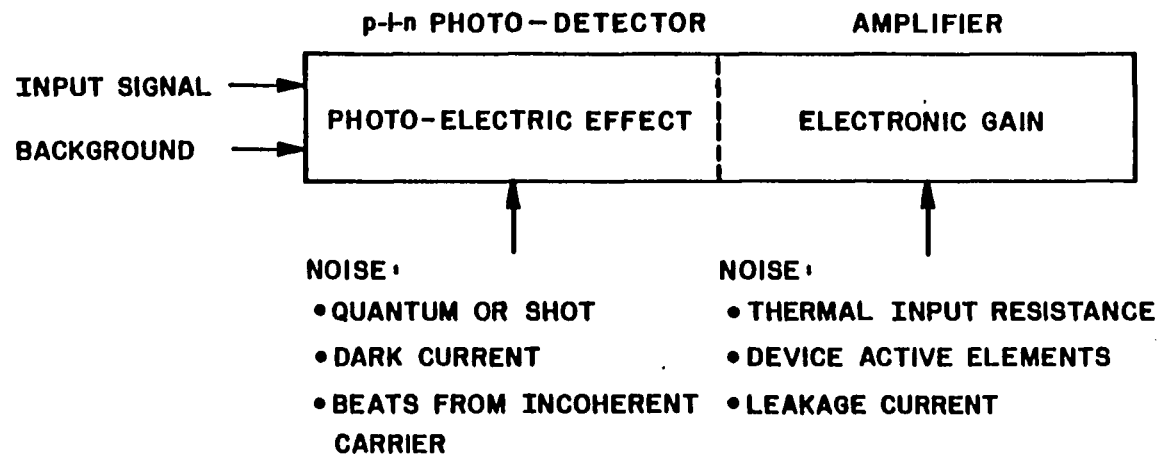
TABLE 1

p-i-n FET Receiver Noise Model Summarization

	Variable	Unit	Theoretical Values		Measured values
			Circuit design values	Values used for good agreement	
Noise coefficients	a	A^2	0.89×10^{-22}	1.87×10^{-22}	5.81×10^{-22}
	b	A^2/Hz	3.65×10^{-26}	3.67×10^{-26}	3.78×10^{-26}
	c	A^2/Hz^2	1.53×10^{-33}	3.21×10^{-33}	3.97×10^{-33}
	d	A^2/Hz^3	1.24×10^{-40}	1.27×10^{-40}	1.16×10^{-40}
Circuit's parameters	C_d	pF	0.50	0.40	0.4 ± 0.1
	C_p	pF	0.20	0.20	0.4 ± 0.2
	C_F	pF	0.10	0.10	0.10 ± 0.05
	C_{gs}	pF	0.50	0.60	0.5 ± 0.1
	C_{gd}	pF	0.02	0.02	0.04 ± 0.02
	g_m	mS	30	30	30 ± 10
	Γ	–	1.61	1.69	1.7 ± 0.1
	P	–	1.24	1.24	1.24 ± 0.01
	f_c	MHz	25	50	10-50
	R_F	kΩ	500	500	$500 + 2\%$
	R_D	Ω	82	82	82
	I_{dn}	nA	10.0	10.7	10.7
	I_{gt}	nA	0.5	0.5	0.1-2.0

TABLE 2

p-i-n BJT Receiver Noise Model Summarization

	Variable	Unit	Theoretical Values		Measured values
			Circuit design values	Values used for good agreement	
Noise Coefficients	a	A^2/Hz	6.90×10^{-24}	6.36×10^{-24}	6.75×10^{-24}
	b	A^2/Hz^3	2.16×10^{-40}	2.64×10^{-40}	2.88×10^{-40}
Circuit's parameters	C_d	pF	0.45	0.50	0.4+0.1
	C_P	pF	0.39	0.39	0.4∓0.2
	C_F	pF	0.01	0.10	0.07∓0.03
	$C_{b'e}$	pF	2.14	2.17	2.1∓0.3
	$C_{b'c}$	pF	0.14	0.14	0.15∓0.04
	h_{fe}	–	118.5	118.5	100∓150
	g_m	mS	58.5	50.6	50-60
	$r_{bb'}$	Ω	25	25	20-30
	$r_{b'e}$	$k\Omega$	2.02	2.33	2.0-3.0
	R_F	$k\Omega$	6.00	6.00	6.00+10%
	R_C	$k\Omega$	2.48	2.48	2.48∓10%
	I_{dn}	nA	10.0	15.0	15.0

p-i-n PHOTO—DETECTOR | AMPLIFIER

INPUT SIGNAL ⟶

BACKGROUND ⟶

PHOTO-ELECTRIC EFFECT | ELECTRONIC GAIN

NOISE:

- QUANTUM OR SHOT
- DARK CURRENT
- BEATS FROM INCOHERENT CARRIER

NOISE:

- THERMAL INPUT RESISTANCE
- DEVICE ACTIVE ELEMENTS
- LEAKAGE CURRENT

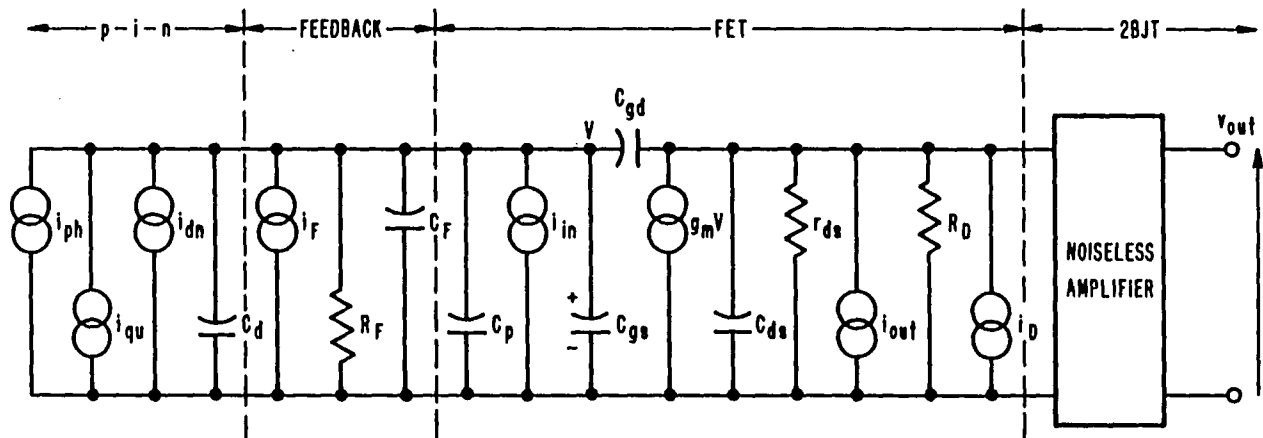NOISE SOURCES AT THE FRONT-END OF AN OPTICAL RECEIVER

FIGURE 1
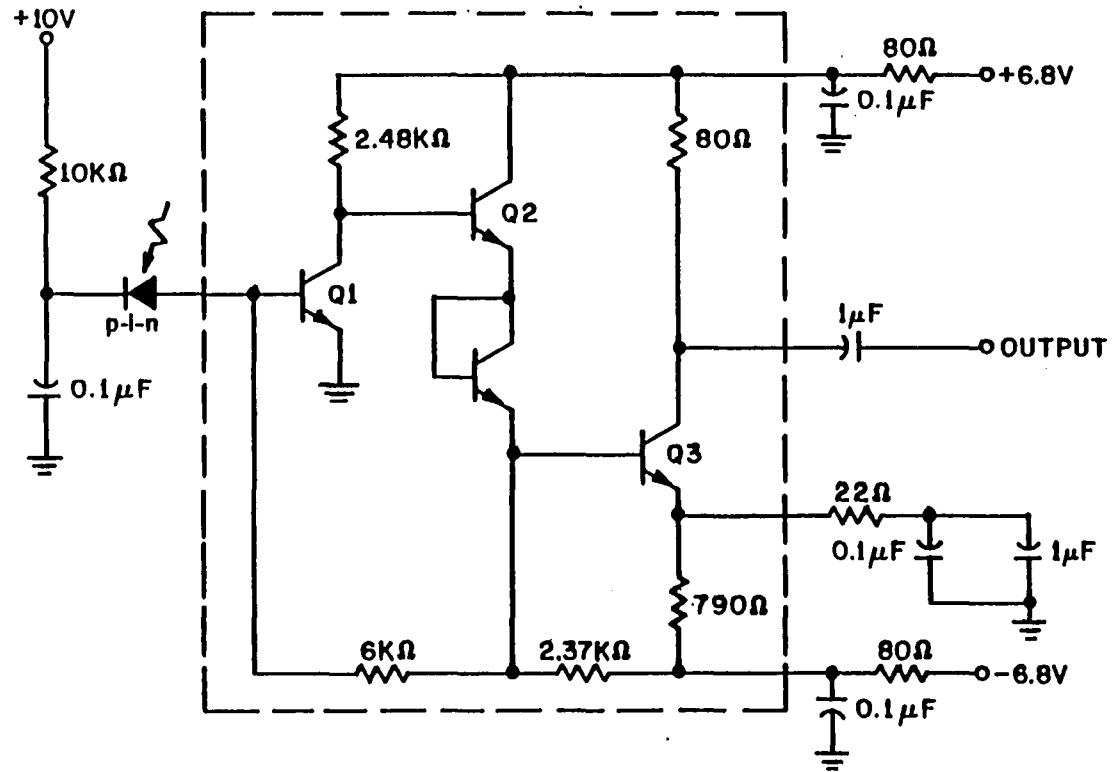
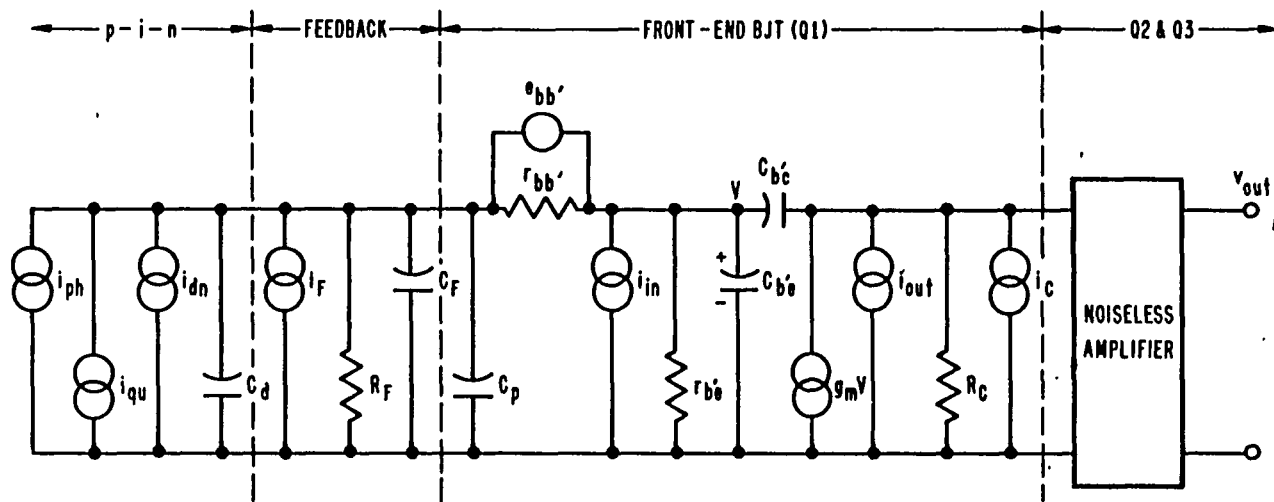1.3 μm p-I-n BJT TRANSIMPEDANCE OPTICAL RECEIVER

FIGURE 3
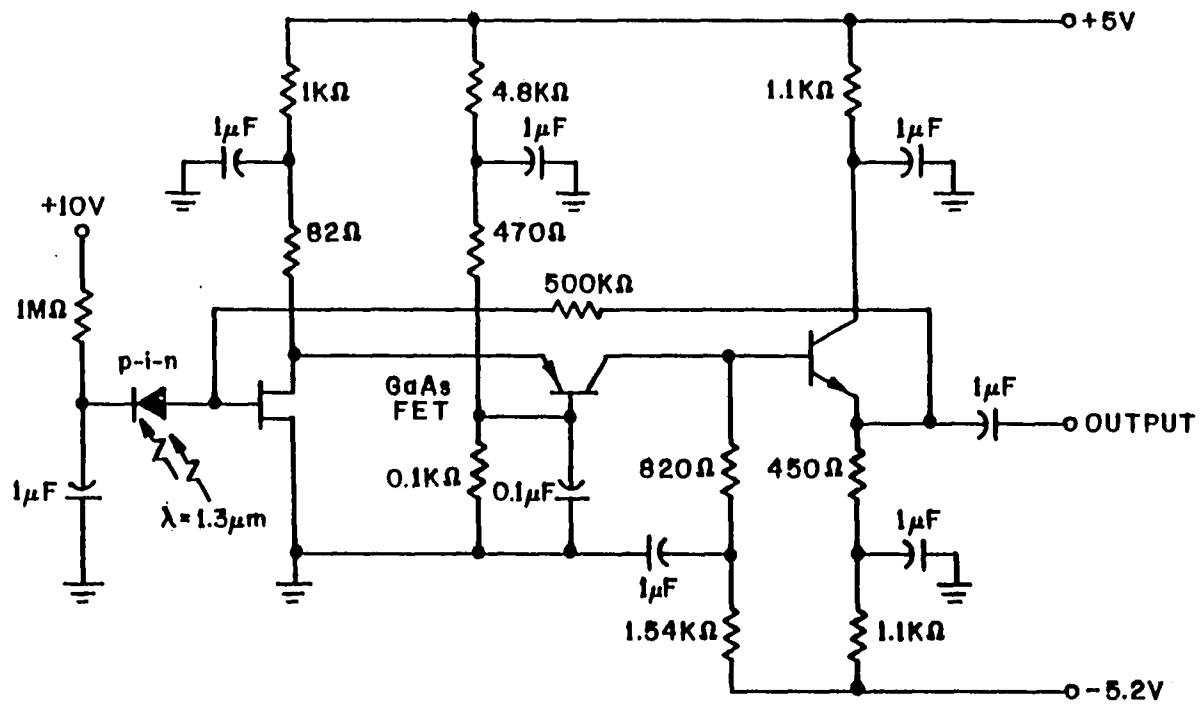
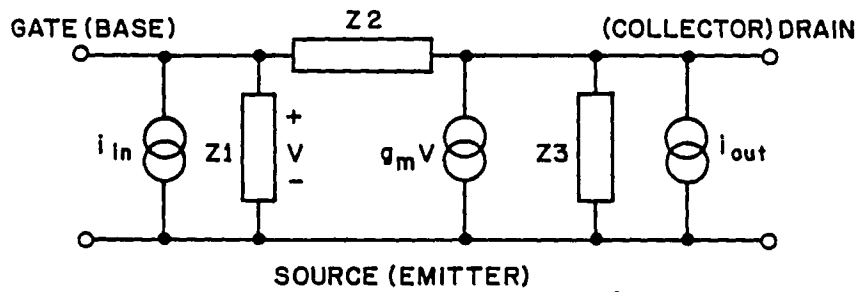1.3μm p-i-n FET TRANSIMPEDANCE OPTICAL RECEIVER

FIGURE 2

1.3μm p-i-n FET OPTICAL RECEIVER NOISE MODEL

FIGURE 4

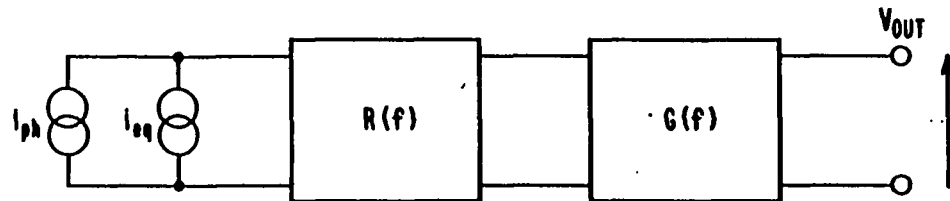1.3μm p-i-n BJT OPTICAL RECEIVER NOISE MODEL

FIGURE 5

STANDARD HYBRID – π NOISE MODEL FOR TRANSISTORS
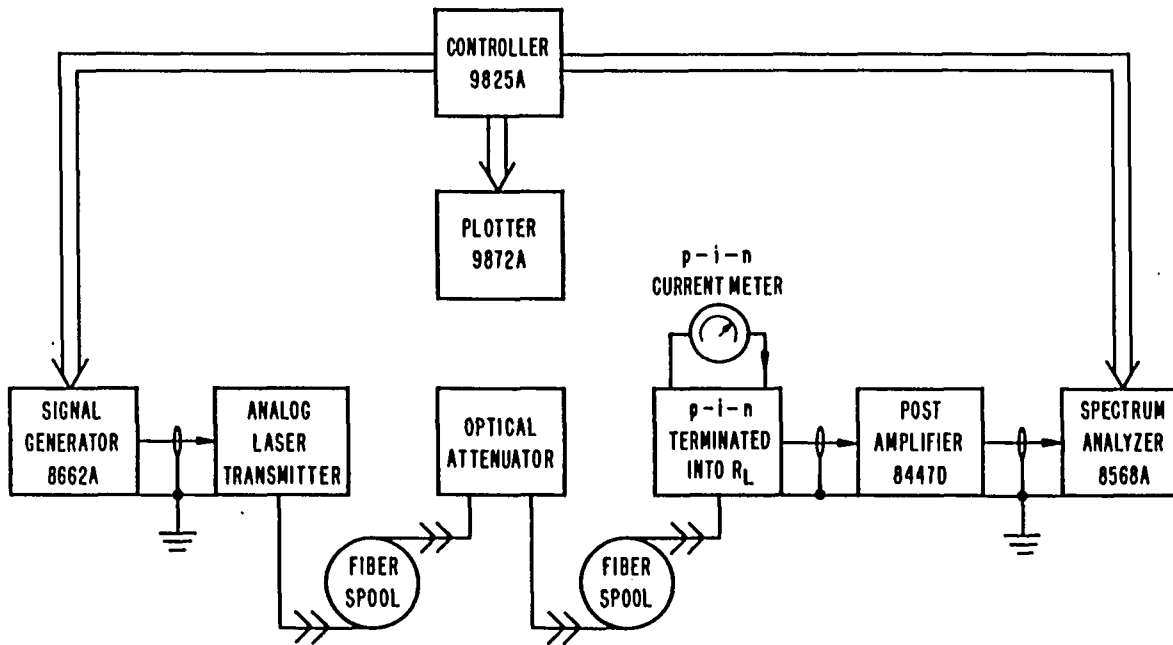
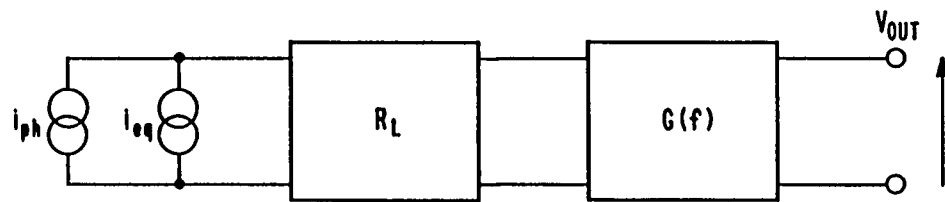FIGURE 6
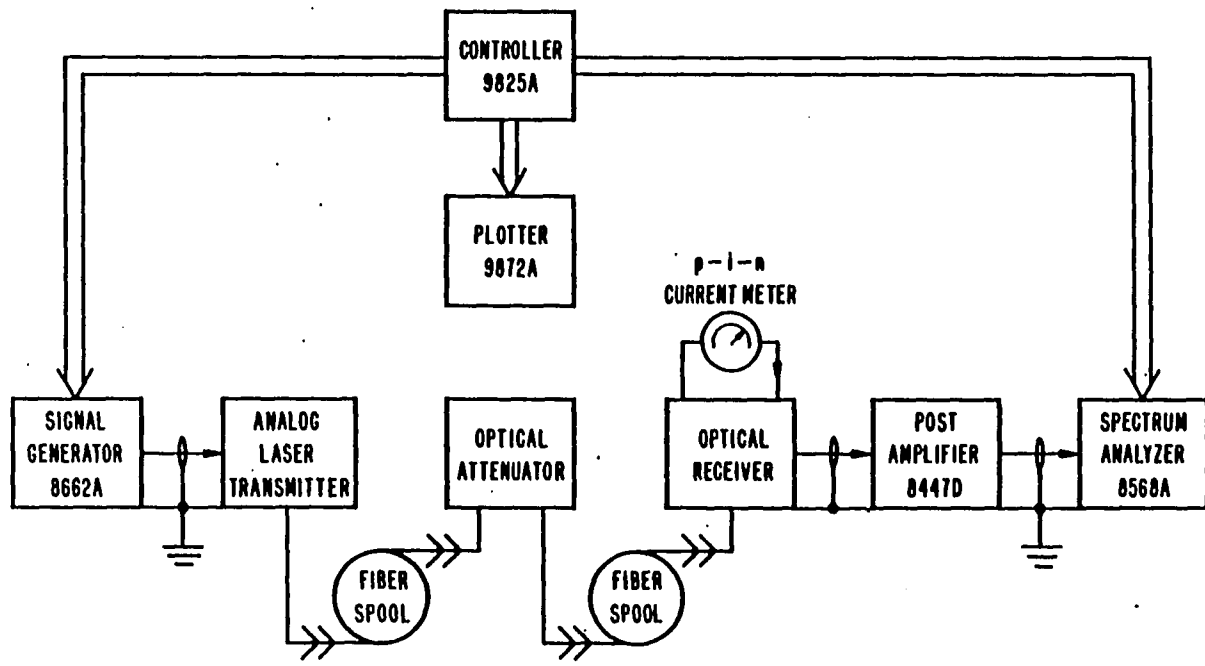
THE EXPERIMENTAL APPARATUS

FIGURE 7

THE EQUIVALENT CIRCUIT OF THE EXPERIMENTAL APPARATUS
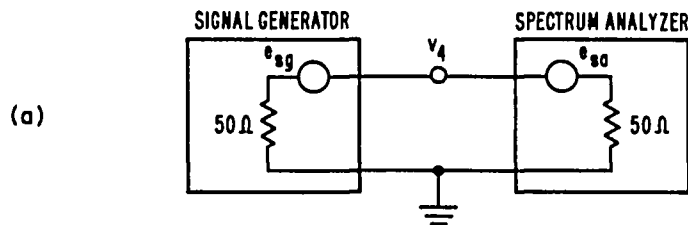AS SEEN BY THE ANALYZER

FIGURE 8

THE APPARATUS USED TO NORMALIZE $\langle i_{ph}^2(f) \rangle$
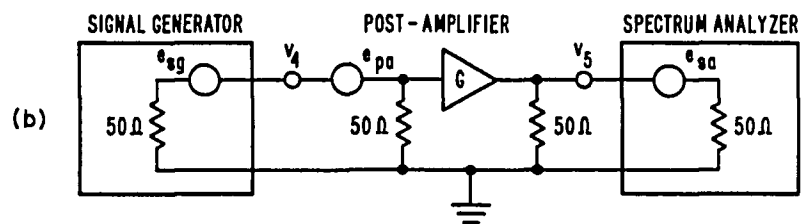
FIGURE 9

THE EQUIVALENT CIRCUIT OF THE APPARATUS
AS SEEN BY THE ANALYZER WHEN $\langle i^2_{ph}(f) \rangle$ IS NORMALIZED

FIGURE 10

(a)

SIGNAL GENERATOR

SPECTRUM ANALYZER

e_{sg}

v_4

e_{sa}

$50\,\Omega$

$50\,\Omega$

$$v_4^2 \gg \langle e_{sg}^2 \rangle + \langle e_{sa}^2 \rangle$$

$$P_4 = 10\log\left(\frac{v_4^2}{50\,\Omega} \times 10^3\right) dBm$$

(b)

SIGNAL GENERATOR

POST-AMPLIFIER

SPECTRUM ANALYZER

e_{sg}

v_4

e_{pa}

G

v_5

e_{sa}

$50\,\Omega$
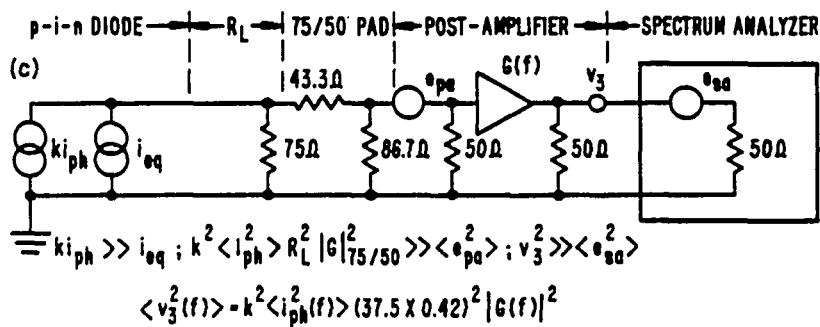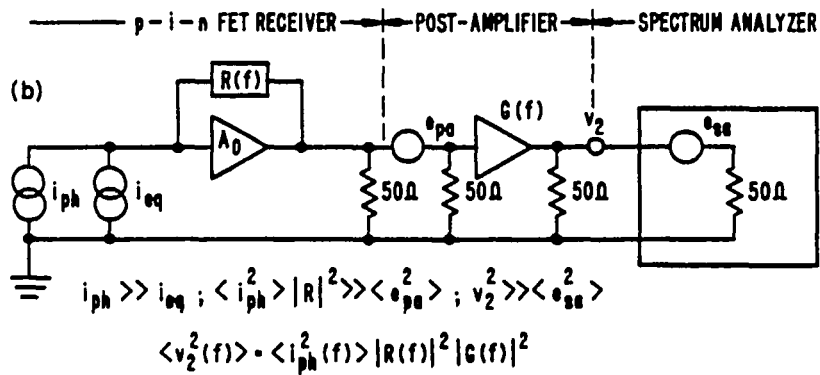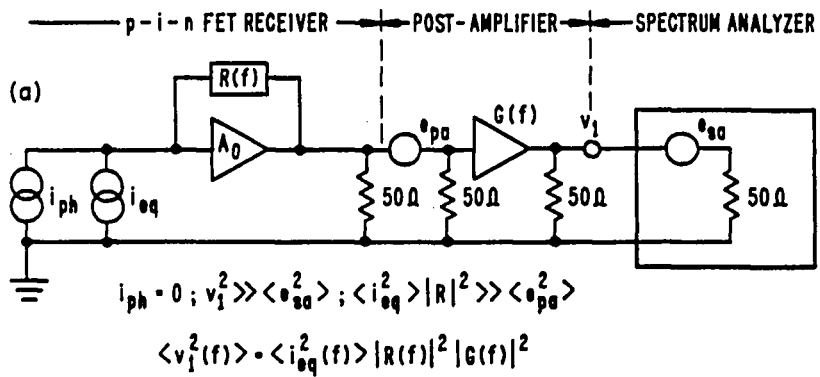
$50\,\Omega$

$50\,\Omega$

$50\,\Omega$

$$v_4^2 \gg \langle e_{sg}^2 \rangle + \langle e_{pa}^2 \rangle$$
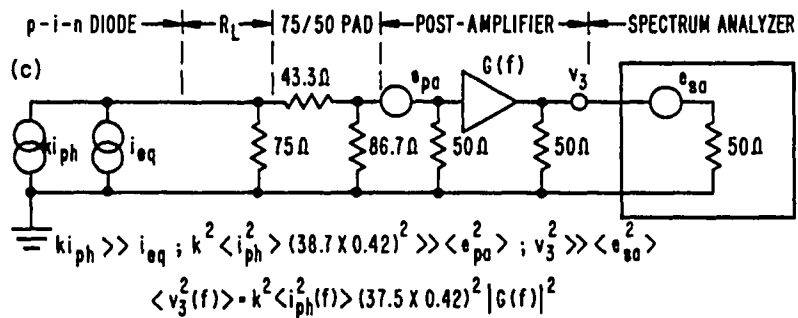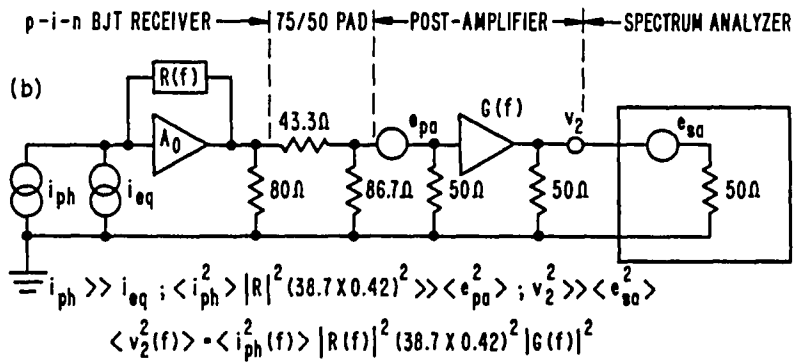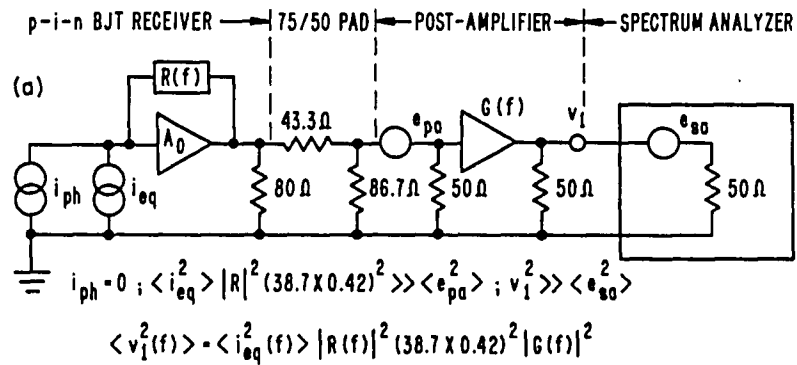
$$v_5^2 \gg \langle e_{sa}^2 \rangle$$

$$P_5 = 10\log\left(\frac{v_5^2}{50\,\Omega} \times 10^3\right) dBm$$

THE EQUIVALENT CIRCUIT USED TO MEASURE
THE POST-AMPLIFIER VOLTAGE GAIN

FIGURE 11

── p – i – n FET RECEIVER ──|──POST–AMPLIFIER──|── SPECTRUM ANALYZER

(a)

$$i_{ph} = 0 \; ; \; v_1^2 \gg \langle e_{sa}^2 \rangle \; ; \; \langle i_{eq}^2 \rangle |R|^2 \gg \langle e_{pa}^2 \rangle$$

$$\langle v_1^2(f) \rangle = \langle i_{eq}^2(f) \rangle |R(f)|^2 |G(f)|^2$$

── p – i – n FET RECEIVER ──|──POST–AMPLIFIER──|── SPECTRUM ANALYZER

(b)

$$i_{ph} \gg i_{eq} \; ; \; \langle i_{ph}^2 \rangle |R|^2 \gg \langle e_{pa}^2 \rangle \; ; \; v_2^2 \gg \langle e_{sa}^2 \rangle$$

$$\langle v_2^2(f) \rangle = \langle i_{ph}^2(f) \rangle |R(f)|^2 |G(f)|^2$$

p – i – n DIODE ──|── R_L ──|── 75/50 PAD ──|──POST–AMPLIFIER──|──SPECTRUM ANALYZER

(c)

$$ki_{ph} \gg i_{eq} \; ; \; k^2 \langle i_{ph}^2 \rangle R_L^2 |G|_{75/50}^2 \gg \langle e_{pa}^2 \rangle \; ; \; v_3^2 \gg \langle e_{sa}^2 \rangle$$

$$\langle v_3^2(f) \rangle = k^2 \langle i_{ph}^2(f) \rangle (37.5 \times 0.42)^2 |G(f)|^2$$

THE EQUIVALENT CIRCUIT DIAGRAMS
FOR THE VARIOUS MEASUREMENTS
WHICH WERE PERFORMED ON THE p–i–n FET RECEIVER
FIGURE 12

p-i-n BJT RECEIVER ──┤75/50 PAD├──POST-AMPLIFIER─┤──SPECTRUM ANALYZER

(a)

$R(f)$

A_0

43.3Ω

$G(f)$

v_1

e_{pa}

e_{sa}

i_{ph} i_{eq} $80\,\Omega$ 86.7Ω $50\,\Omega$ $50\,\Omega$ $50\,\Omega$

$i_{ph} = 0$; $\langle i_{eq}^2 \rangle |R|^2 (38.7 \times 0.42)^2 \gg \langle e_{pa}^2 \rangle$; $v_1^2 \gg \langle e_{sa}^2 \rangle$

$\langle v_1^2(f) \rangle = \langle i_{eq}^2(f) \rangle |R(f)|^2 (38.7 \times 0.42)^2 |G(f)|^2$

p-i-n BJT RECEIVER ──►┤75/50 PAD├──POST-AMPLIFIER─►┤──SPECTRUM ANALYZER

(b)

$R(f)$

A_0

43.3Ω

$G(f)$

v_2

e_{pa}

e_{sa}

i_{ph} i_{eq} $80\,\Omega$ 86.7Ω $50\,\Omega$ $50\,\Omega$ $50\,\Omega$

$i_{ph} \gg i_{eq}$; $\langle i_{ph}^2 \rangle |R|^2 (38.7 \times 0.42)^2 \gg \langle e_{pa}^2 \rangle$; $v_2^2 \gg \langle e_{sa}^2 \rangle$

$\langle v_2^2(f) \rangle = \langle i_{ph}^2(f) \rangle |R(f)|^2 (38.7 \times 0.42)^2 |G(f)|^2$

p-i-n DIODE ──►┤── R_L ──►┤75/50 PAD├──POST-AMPLIFIER──►┤──SPECTRUM ANALYZER

(c)

43.3Ω

$G(f)$

v_3

e_{pa}

e_{sa}

$k i_{ph}$ i_{eq} $75\,\Omega$ 86.7Ω $50\,\Omega$ $50\,\Omega$ $50\,\Omega$

$k i_{ph} \gg i_{eq}$; $k^2 \langle i_{ph}^2 \rangle (38.7 \times 0.42)^2 \gg \langle e_{pa}^2 \rangle$; $v_3^2 \gg \langle e_{sa}^2 \rangle$

$\langle v_3^2(f) \rangle = k^2 \langle i_{ph}^2(f) \rangle (37.5 \times 0.42)^2 |G(f)|^2$

THE EQUIVALENT CIRCUIT DIAGRAMS
FOR THE VARIOUS MEASUREMENTS
WHICH WERE PERFORMED ON THE p-i-n BJT RECEIVER
FIGURE 13

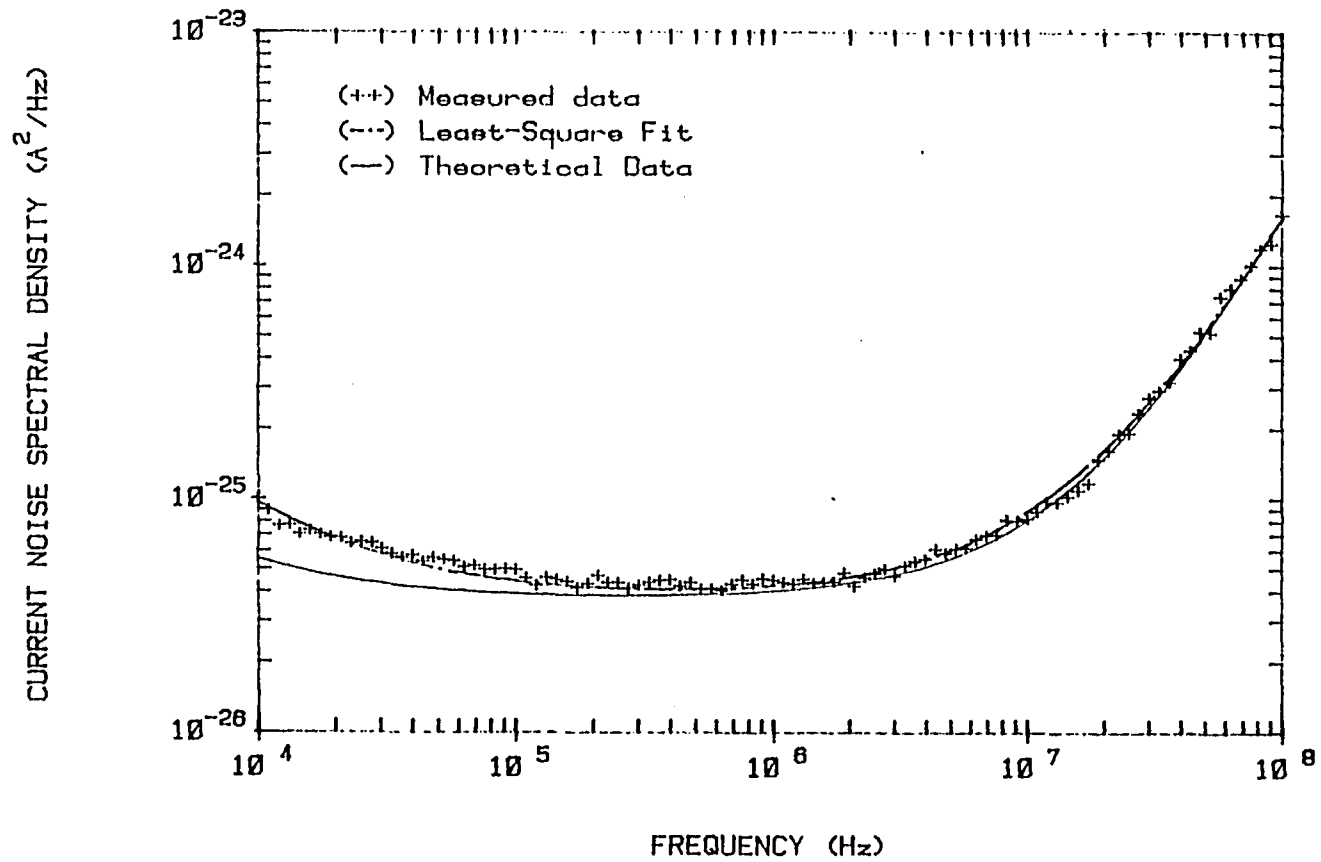PIN-FET RECEIVER EQUIVALENT INPUT CURRENT NOISE SPECTRAL DENSITY
04/30/83 TVN

FIGURE 14

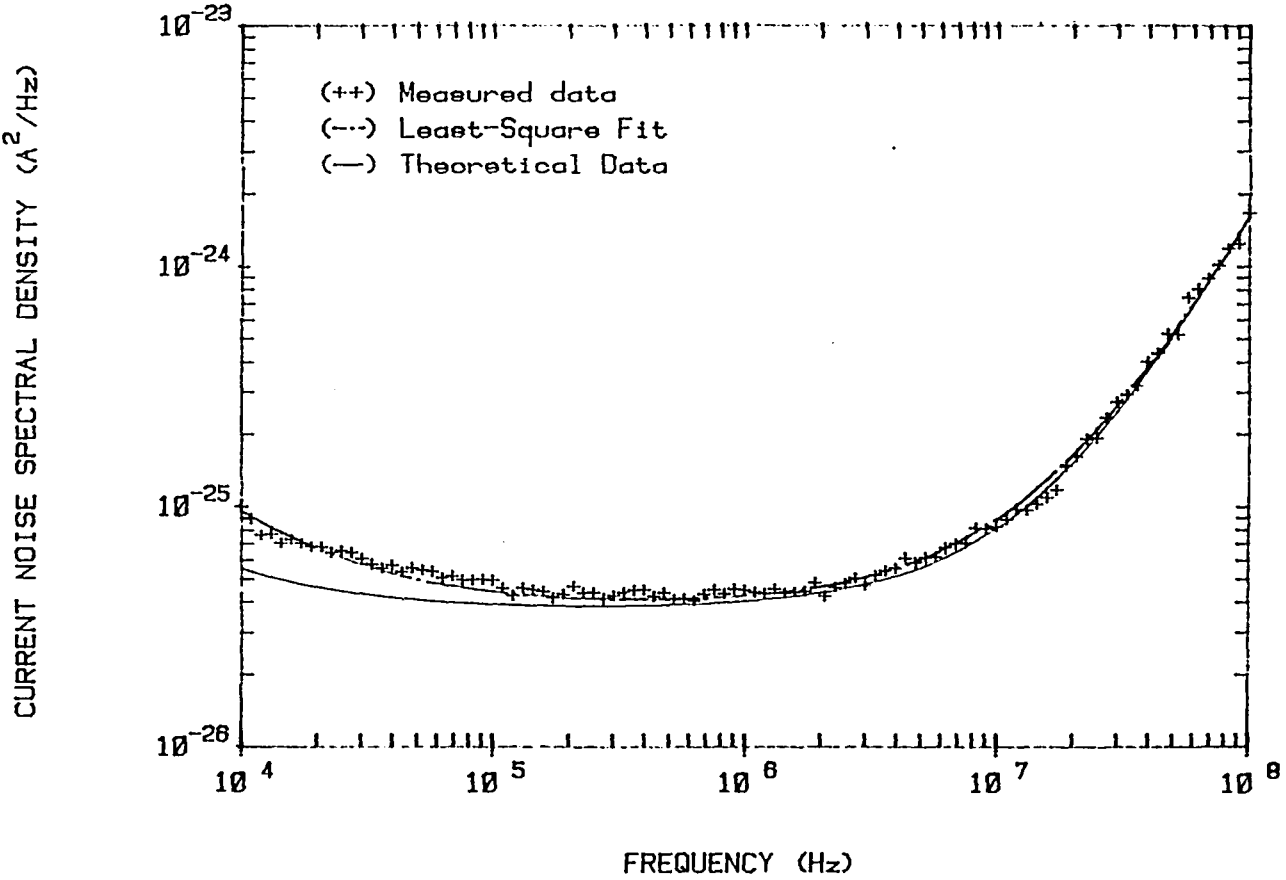PIN-FET RECEIVER EQUIVALENT INPUT CURRENT NOISE SPECTRAL DENSITY
04/30/83 TVN

FIGURE 14

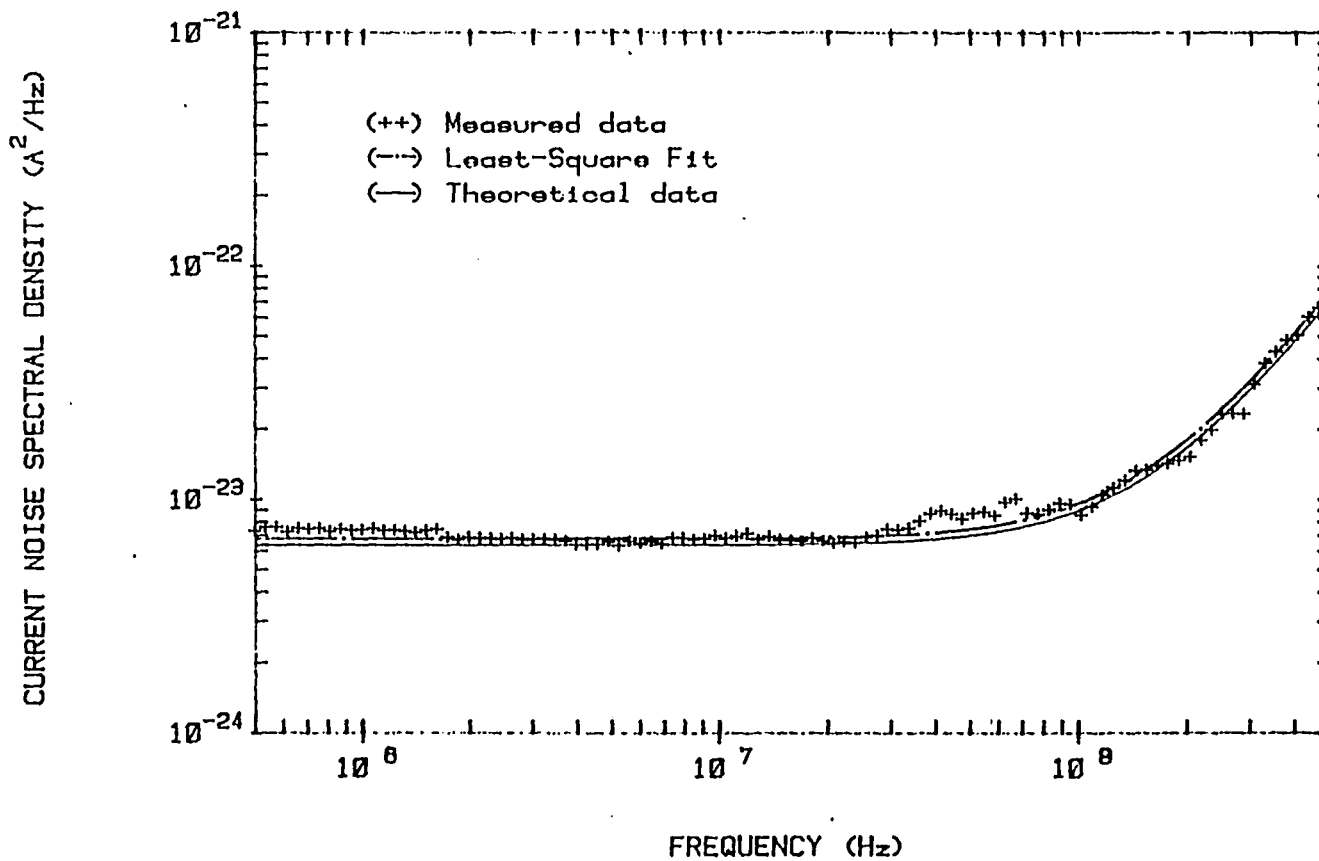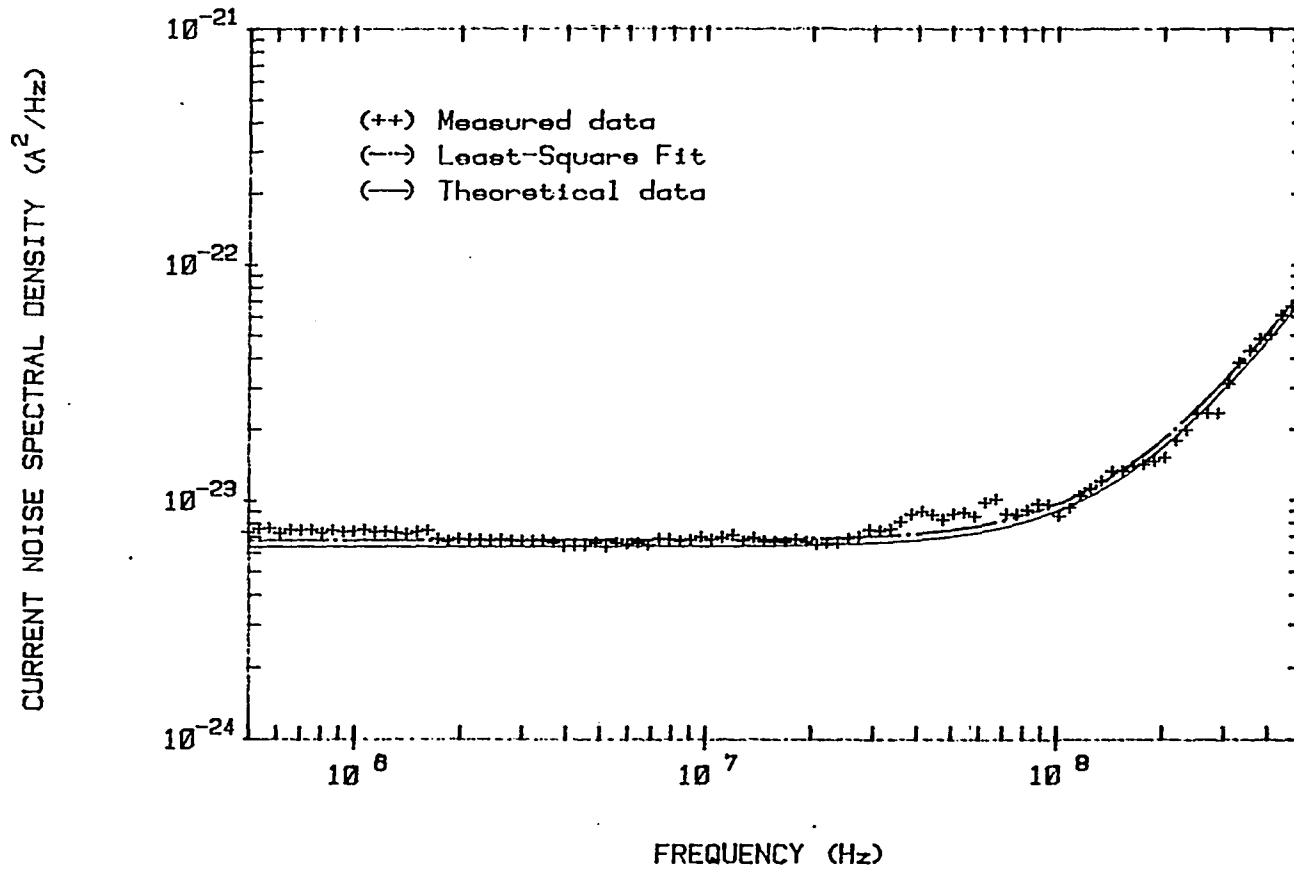PIN-BJT RECEIVER EQUIVALENT INPUT CURRENT NOISE SPECTRAL DENSITY
05/12/83 TVN

(++) Measured data
(--) Least-Square Fit
(—) Theoretical data

FIGURE 15

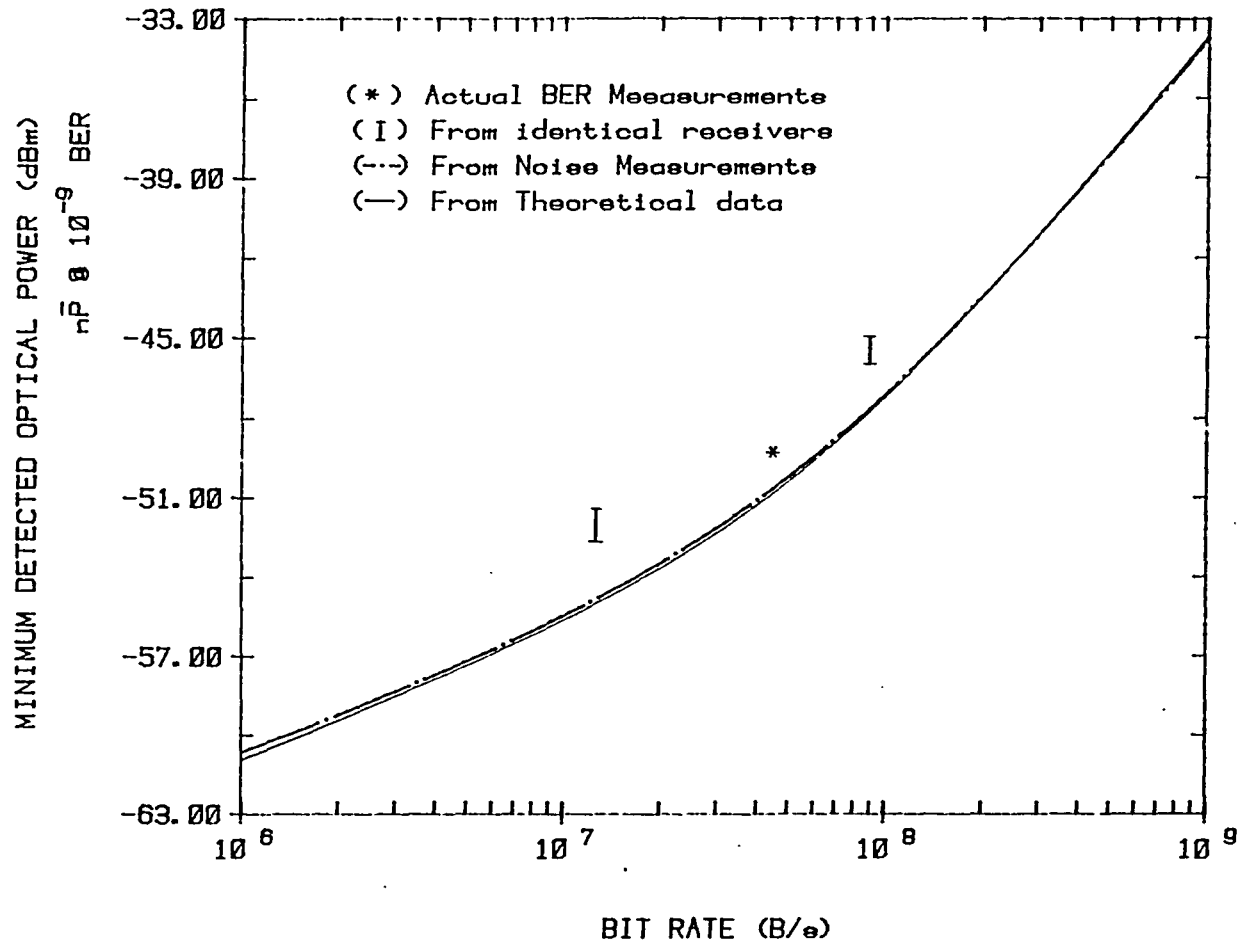PIN-BJT RECEIVER EQUIVALENT INPUT CURRENT NOISE SPECTRAL DENSITY

05/12/83 TVN

FIGURE 15

PIN-FET RECEIVER SENSITIVITY AS A FUNCTION OF TRANSMISSION BIT RATE
04/30/83 TVN
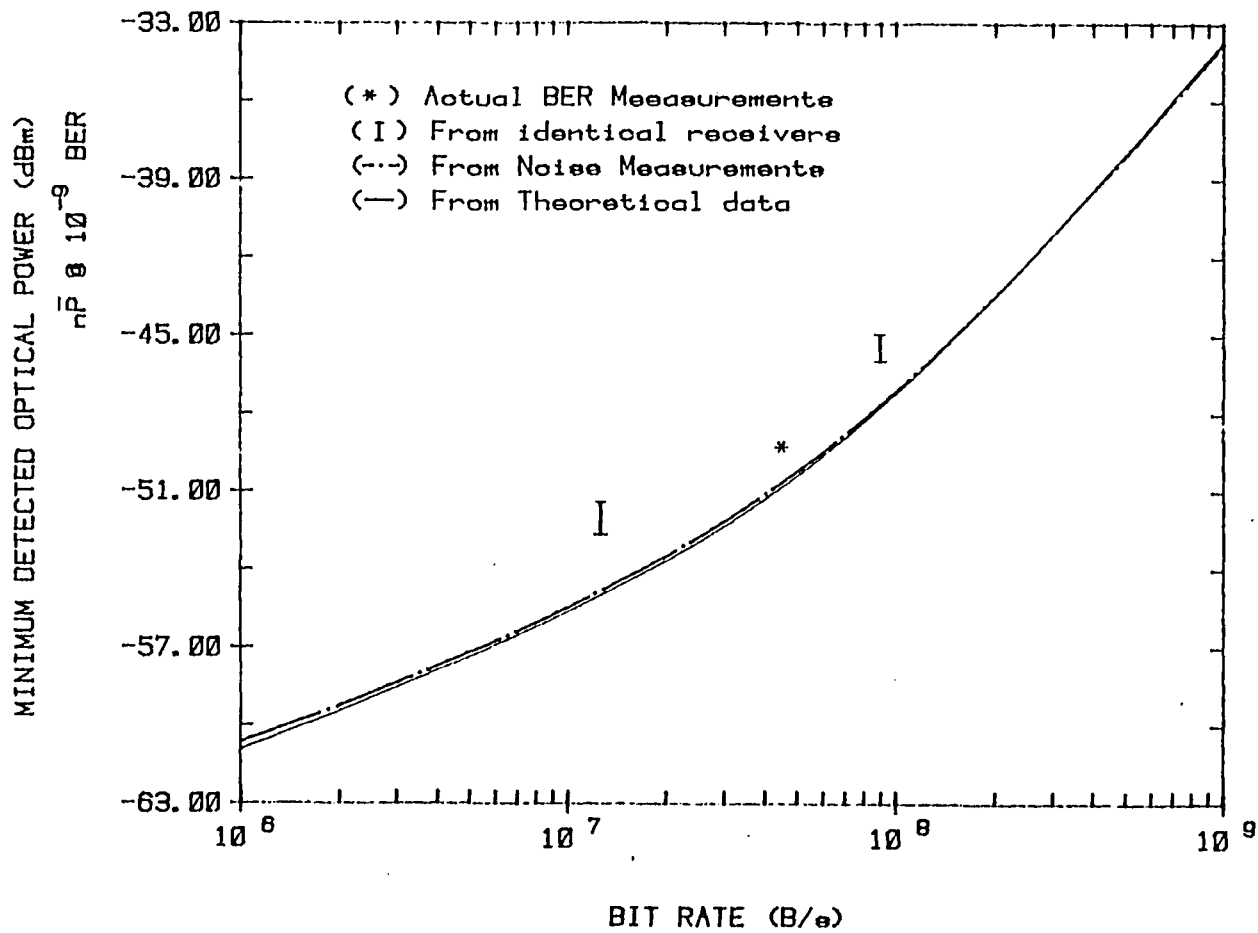
FIGURE 16

PIN-FET RECEIVER SENSITIVITY AS A FUNCTION OF TRANSMISSION BIT RATE
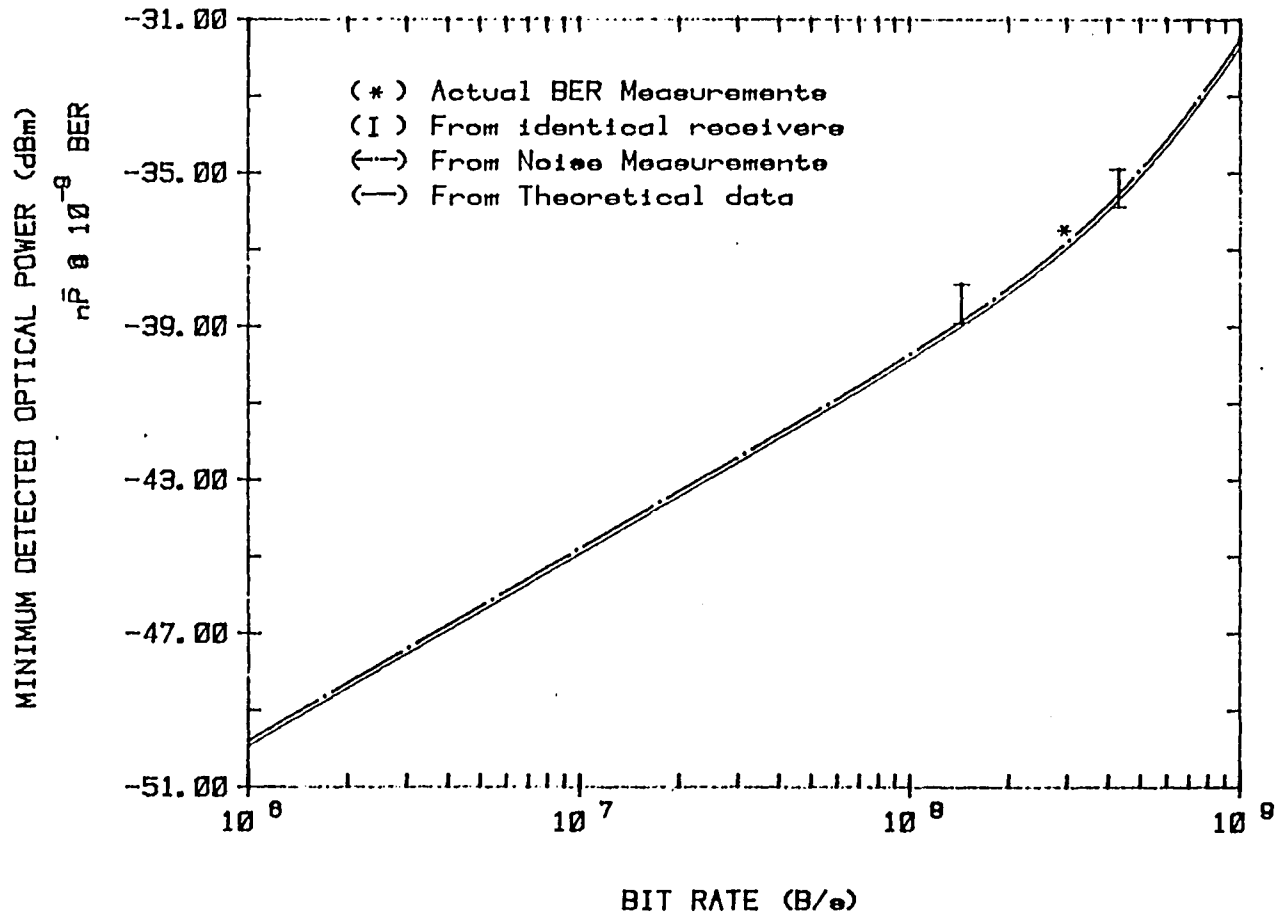04/30/83 TVN

(*) Actual BER Measurements
(I) From identical receivers
(---) From Noise Measurements
(—) From Theoretical data

BIT RATE (B/s)

FIGURE 16

PIN-BJT RECEIVER SENSITIVITY AS A FUNCTION OF TRANSMISSION BIT RATE

05/12/83 TVN

FIGURE 17

PIN-BJT RECEIVER SENSITIVITY AS A FUNCTION OF TRANSMISSION BIT RATE

(*) Actual BER Measurements
(I) From identical receivers
(←→) From Noise Measurements
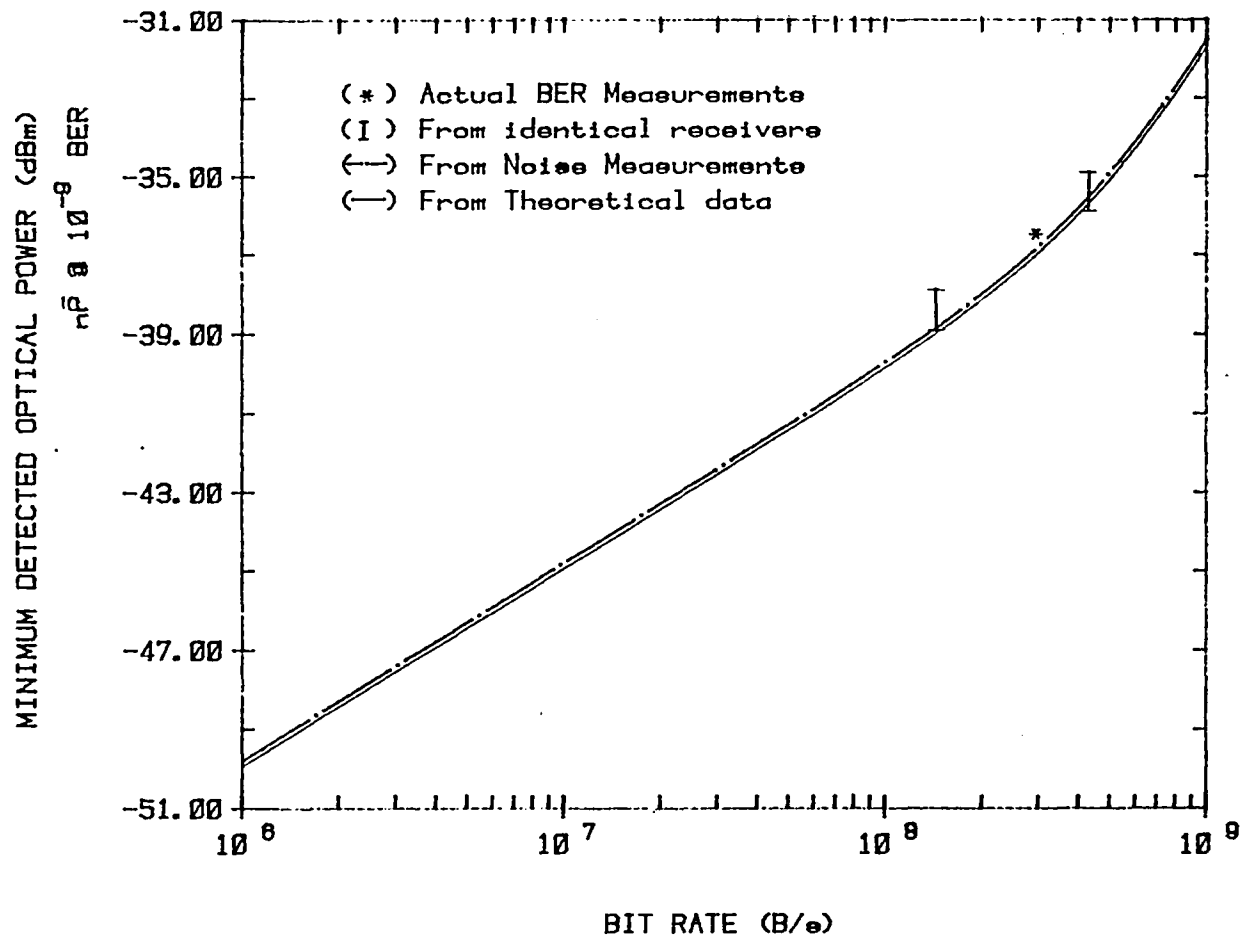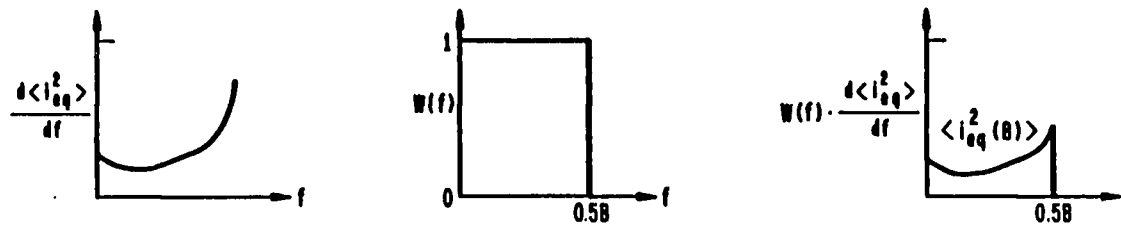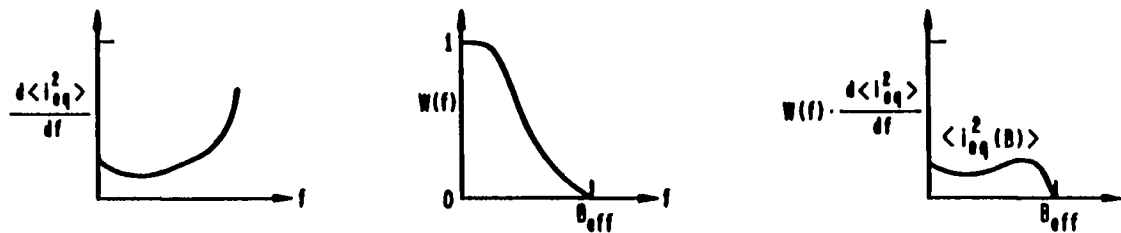(——) From Theoretical data

FIGURE 17

(a) THE CASE OF IDEAL SYSTEM FILTER BAND-SHAPE

(b) THE CASE OF PRACTICAL SYSTEM FILTER BAND-SHAPE

GRAPHICAL PRESENTATION OF THE EQUIVALENT INPUT MEAN SQUARE NOISE CURRENT
AS A FUNCTION OF THE SYSTEM FILTER BAND-SHAPE

FIGURE 18